HERON

Volume 49, no. 4

Delft University Press / 2004

This publication is named after HERON of Alexandria, a Greek scientist, physicist and geometrician who lived in the first century AD. His all-round knowledge came to us through a number of his writings, in which he dealt with mechanics, hydraulic presses and mechanical systems. HERON was also adept at constructing intriguing automatic devices, in which he made ingenious use of physical laws governing the flow of liquids and gases.
The combination of knowledge and practical ingenuity which this ancient engineer (in the true sense of the word) had at his command is still an essential condition for performing present-day research. The cover depicts the statue of HERON.

Contents HERON, 49, no. 4 (2004)

An economic method to determine the strength class of wood species

Geert Ravenshorst[1], Mario van der Linden[1], Ton Vrouwenvelder[1] and Jan-Willem van de Kuilen[2, 3]

[1] TNO Building and Construction Research, Delft, The Netherlands

[2]. Delft University of Technology, Delft, The Netherlands

[3] CNR-Ivalsa, Italy

As a result of the demand for wood from forests that are managed in an environmentally sustainable manner, many unknown wood species are introduced into the market at the moment. To classify a wood species into a strength class and determine the accompanying grading parameters for visual grading in practice, the strength characteristics are traditionally determined by destructive tests, with a minimum of 40 test pieces. To support a quick introduction of unknown wood species a method has been developed in which only 25% of the test sample that is investigated has to be tested destructively, and 75% can be tested non-destructively. This approach is more economic and faster than the present traditional method. This method has been developed by obtaining general correlations that are species-independent between non-destructive measured timber characteristics and the timber strength.

Keywords: timber strength, non-destructive measurements, timber strength modelling

1 Introduction

Different wood species have different strength characteristics, and also within a species these characteristics may vary. Therefore, in practice, a classification system of strength classes is used. Beams from a wood species that fulfil some predefined visual or machine measured characteristics are assigned (graded) into an accompanying strength class for practical application.

In figure 1 a scheme is given of the different steps necessary before grading of beams from a new, unknown species is possible. The procedure is as follows: one or more representative samples of the species are selected. The number of samples depends on the number of grades one wishes to use for the species in practice. When visual grading is intended, the different grades are characterised by visual characteristics such as knot sizes. Different visual grades then have different limitations for the allowable knot sizes: the higher the grade, the smaller the knots sizes that are allowed. The strength properties (bending strength, modulus of elasticity and density) of the beams of the samples are determined by testing. Traditionally, the bending

strength is determined by destructive testing. Based on the test results the characteristic values of the strength properties have to be determined for a test sample. For the bending strength the characteristic value is the 5%-lower limit. The characteristic values are compared with those of the European strength class system [2]. When the characteristic values are higher than those of a specific strength class, than that strength class is assigned to the grade of the test sample. For use in practice it is documented to which strength class a specific visual grade is connected.
For machine grading the procedure is basically the same; the only difference is that the properties of a grade like the density or the modulus of elasticity of the beams are measured by a machine. After the testing and classification the grading rules are incorporated in the settings of the machine for its use in practice.

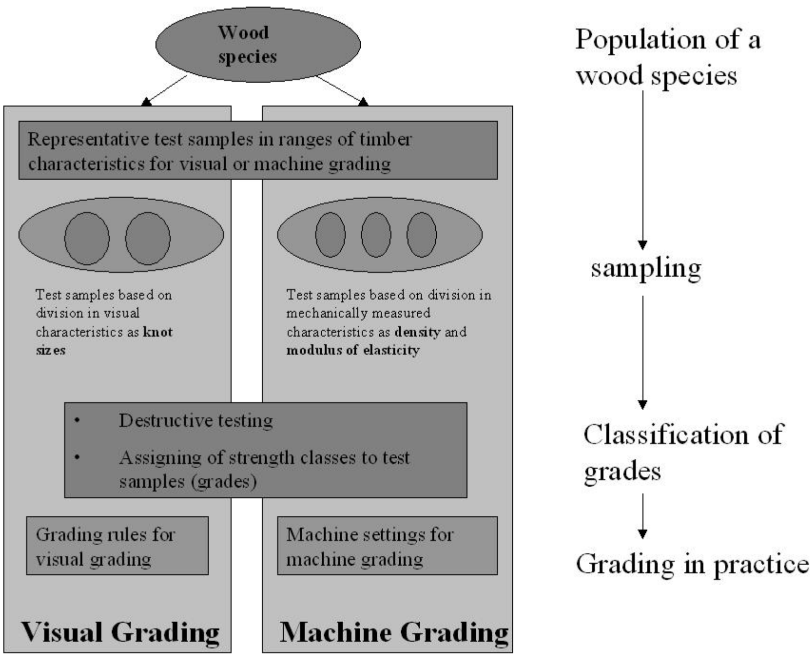

Figure 1: Scheme for necessary testing to determine grading rules for visual or machine grading of beams from a wood species

Presently many unknown wood species are introduced into the market as a result of the demand for timber from forests that are managed in a sustainable, environmentally friendly manner. To be able to use them in building structures the strength has to be known. To classify a wood species into a strength class, the strength characteristics are traditionally determined by destructive tests, as is pointed out in figure 1 in the box "classification of grades". This procedure is time-consuming and expensive. For that reason, it has been investigated, if, using

historical data, general relations could be found between certain non-destructive measured timber properties and timber strength for different wood species. As a result the number of destructive tests needed for new wood species could be limited.
To achieve this goal, it is necessary to formulate models through which, after the processing of the non-destructive and destructive test results, the 5%-lower limit strength can be calculated. In this paper a model is being presented and illustrated by test results. With the presented model, visual grades of a new unknown (hardwood) species can be classified into a strength class using less destructive tests than is necessary when using the traditional method.
As will be explained later, for most hardwood timber only one visual grade can be distinguished. Machine grading however, is more accurate and offers the possibility of having more grades. For this reason TNO developed a mobile strength grading device that makes this possible in practice. This will be outlined shortly in section 7, future developments.

Figure 2: A lot of 'new' wood species are introduced onto the market today

2 Backgrounds regarding the determination of the strength-properties of timber

2.1 General

To design timber structures it is necessary to know the strength properties of the species to be used. To determine these properties a representative sample of the wood species has to be tested. To assign the derived properties to individual beams of these species the characteristics of the tested sample have to be set up. In Europe a system of strength classes is adopted, whereby a complete set of property-values is represented by one mark [2]. Based on the tested sample, beams of a wood species that fulfil the requirements for the characteristics can be connected to a strength class.

A basic principle is that the strength class can be determined by three main properties: the bending strength, the modulus of elasticity and the density. For the bending strength and the density the 5%-lower fractile has to be determined and for the modulus of elasticity the mean value.

2.2 Grading of timber. Material predicting properties. Visual/machine grading

In practice, the timber beams of a species are graded according to the characteristics that have been set up during an initial testing procedure. The grading procedure prescribes the growth characteristics that are used. For visual grading, characteristics as knot size and knot ratio are the main parameters. The limit values for these characteristics are laid down in grades, published in standards. A grade of a wood species can be connected to a strength class. For machine grading, parameters as modulus of elasticity and density are used to select the beams. The grading parameters are used for both methods, visual and machine grading, to predict the strength properties of the sorted beams. As a result of the grading process no more than 5% of the beams may incorrectly be graded too high.

The principle of predicting the bending strength by visual and machine grading is illustrated in figures 3 and 4. These figures are representative for a softwood species. In figure 3 a typical correlation diagram for the knot ratio and the bending strength is presented. The limits on the horizontal axes indicate the different grades. Using the requirement that no more than 5% of the beams in a grade class may incorrectly be upgraded, the exact limits for these grades can be established depending on the classification values for the bending strength on the vertical axis. The 5% incorrectly upgraded beams are marked by the black triangles in the figure. In figure 4 a typical correlation between the modulus of elasticity and the bending strength is shown. This property is often used in machine grading, where the modulus of elasticity is determined either by leading the beams through a bending machine or by means of a longitudinal stress wave analysis. Figures 3 and 4 show that the modulus of elasticity is a more accurate grading property for the bending strength than the knot ratio. As a result, using the modulus of elasticity as a grading property makes it possible to grade beams in a higher strength class.

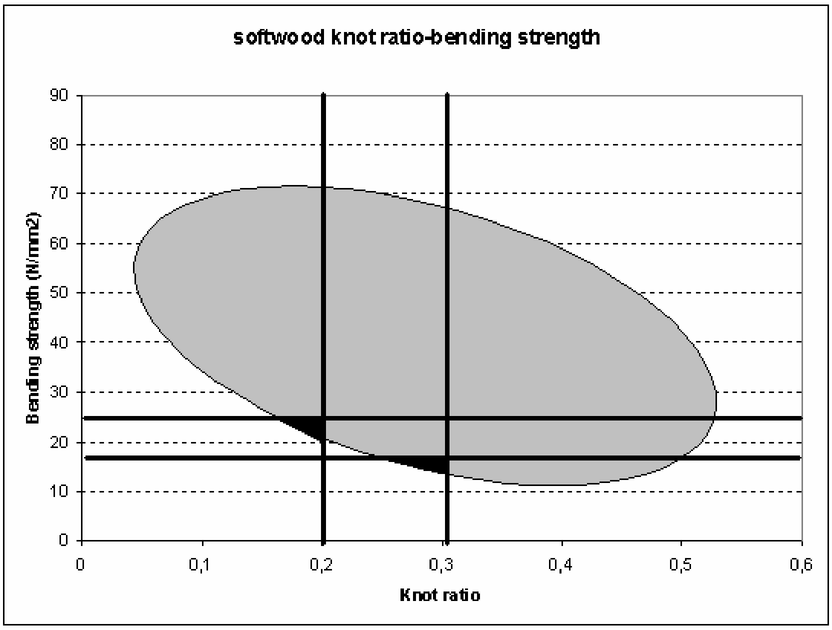

Figure 3: Typical correlation diagram for a softwood species between knot ratio and bending strength

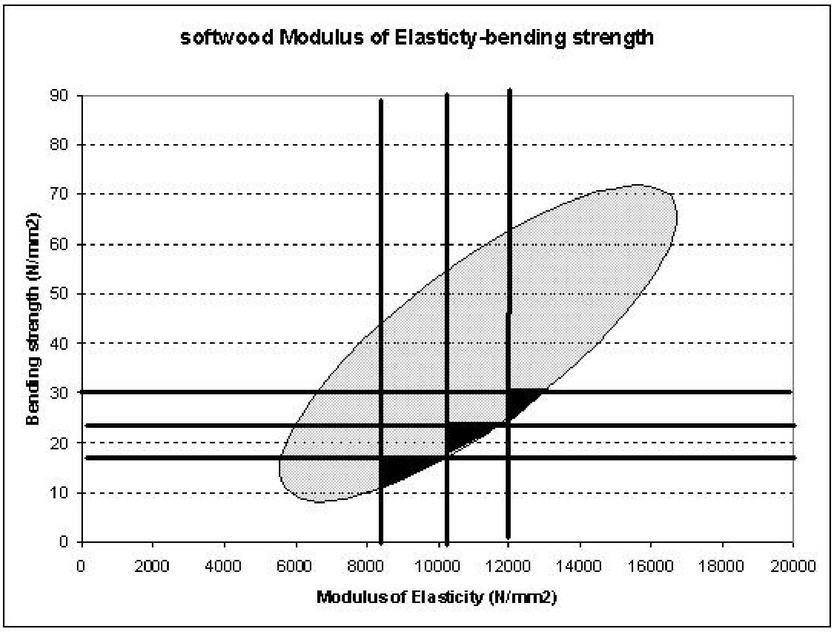

Figure 4: Typical correlation diagram for a softwood species between Modulus of Elasticity and bending strength

2.3 Classification methods. Number of tests. Use of Non-parametric distribution

The strength properties for a population (a grade or a species/ grade combination) are derived from a representative sample from this population. In the European standards a population is defined as a material for which the characteristic values are relevant. The population can be defined by parameters such as species, species grouping or source. According to the European standards prEN14081-1 [1] and EN 384 [3] a minimum of 40 representative beams have to be tested for each sorting grade of the population. Traditionally all 40 beams are tested destructively in a four-point bending test according to EN 408 [4].

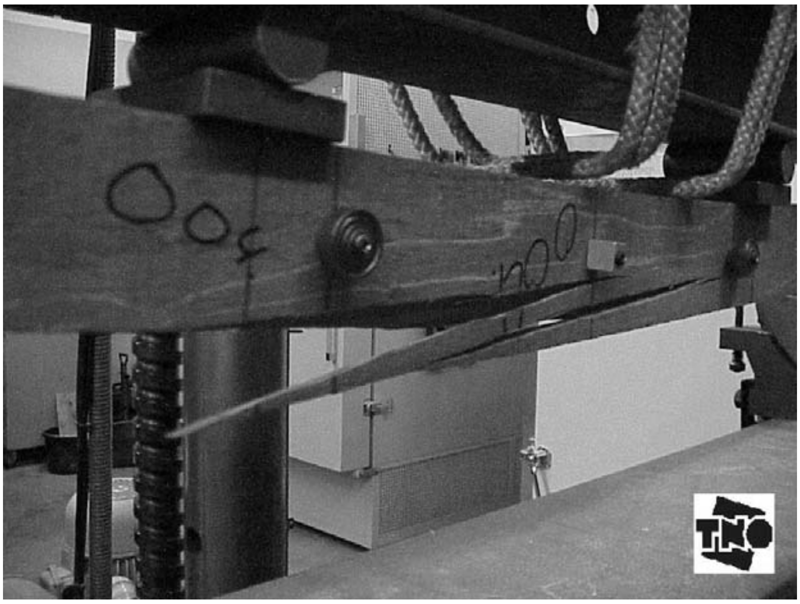

Figure 5: Four-point bending test according to EN 408

The 5%-fractile of the bending strength has to be determined by a non-parametric evaluation of the test results. This means that test results are ranked in order of their value. The 5%-fractile value indicates that 5% of the tests give lower values. For example, after ranking the test values of a sample size of 100, the fifth test value is the 5%-fractile value of the sample.
In general, the first reason for using non-parametric tests is that the actual distribution of the test results may be unknown. The second reason is that by performing extensive tests (say more than 300), it has been proven that a 5%-fractile of both the non-parametric distribution and the normal distribution is almost the same. For a smaller number of tests, like 40 as required for a new species, the reliability of the prediction can be improved if the distribution is known and a parametric method is used. This approach has been followed in this research.

2.4 Testing methods. Standardized methods and alternative methods.

To perform tests for bending strength, modulus of elasticity and density, standardized methods are described in the European standards EN 384 [3] and EN 408 [4], respectively. When other test methods are used they have to be adjusted to the reference conditions described in the standards mentioned. The standardized test methods for both the determination of the bending strength and the modulus of elasticity are described in section 2.4.1 Alternative methods are described in section 2.4.2.

2.4.1 Determination of the bending strength and modulus of elasticity by standardized tests.

The bending strength and the modulus of elasticity are determined by a four-point bending test. The modulus of elasticity is calculated out of the measured deflection at a force between 10% and 40% of the failure force. The modulus of elasticity derived in this way is called the static modulus of elasticity.

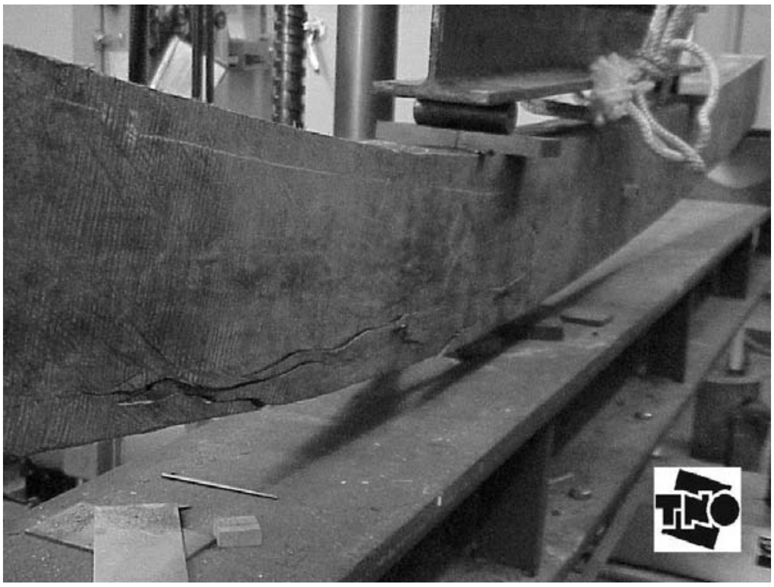

Figure 6: The static modulus of elasticity is calculated out of the deflections measured in a four-point bending test according to EN 408.

2.4.2 Determination of the bending strength and modulus of elasticity by alternative testing methods.

The modulus of elasticity may be derived by measuring the frequency response. This principle is described in [5]. The modulus of elasticity determined this way is called the dynamic modulus of elasticity. The dynamic modulus of elasticity has shown to have a strong correlation

with the static modulus of elasticity. In this research, a device developed by TNO, the Mobile Timber Grader was used to derive the dynamic modulus of elasticity.
The bending strength can also be calculated on the basis of non-destructive measurements, when models to predict the bending strength are formulated. This will be presented in section 4 of this paper.

3 Research programme

3.1 Scope of the research

Nowadays "new" hardwood wood species are introduced into the market as a result of the demand for timber from forests that are managed in an environmentally sustainable manner. The strength properties of these "new" species are not known and have to be determined. Therefore the demand rose for an economic method to determine the strength class of these "new" wood species. The research programme included two goals:

- The first goal was to develop an economic method with combined destructive and non-destructive tests for the classification of "new" wood species in a strength class, in combination with visual grading.
- The second goal was to study the possibility of optimising the grading of beams of a hardwood species into more than one strength class, when the beams are machine graded.

To illustrate the second goal figures 7 and 8 will be discussed. These figures can be compared with figures 3 and 4 for softwood species. The knot ratio and the bending strength for a tropical hardwood species with less visual distinct characteristics as knots, is presented as a typical correlation diagram in figure 7. Figure 8 shows a typical correlation pattern of the modulus of elasticity and the bending strength of this tropical hardwood species. For both figures the black fills mark the 5% incorrectly upgraded beams. These figures show that, in contradiction with the softwood example, it is not possible to distinct more than one economic interesting grade based on both the knot ratio and the modulus of elasticity. For the knot ratio this can be explained by the fact that most tropical hardwood species have no clear visual characteristics such as knots.

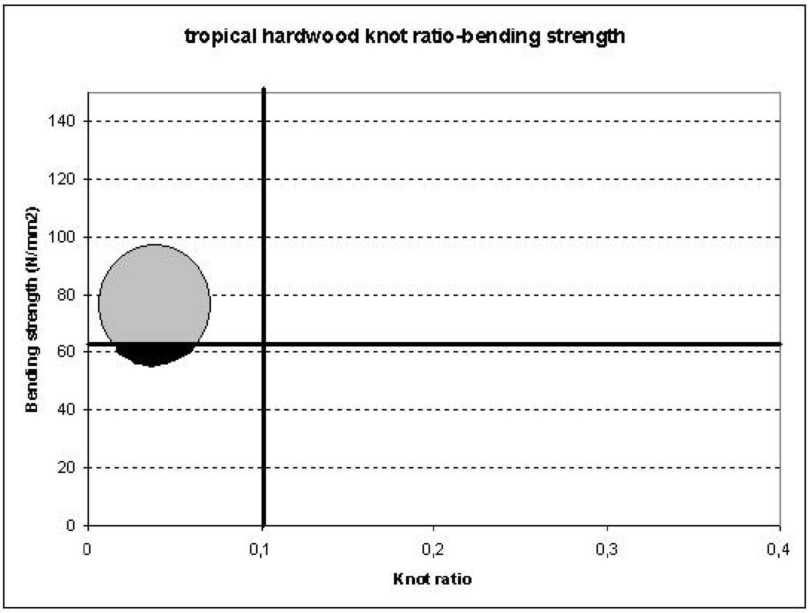

Figure 7: Typical correlation diagram for a hardwood species between knot ratio and bending strength

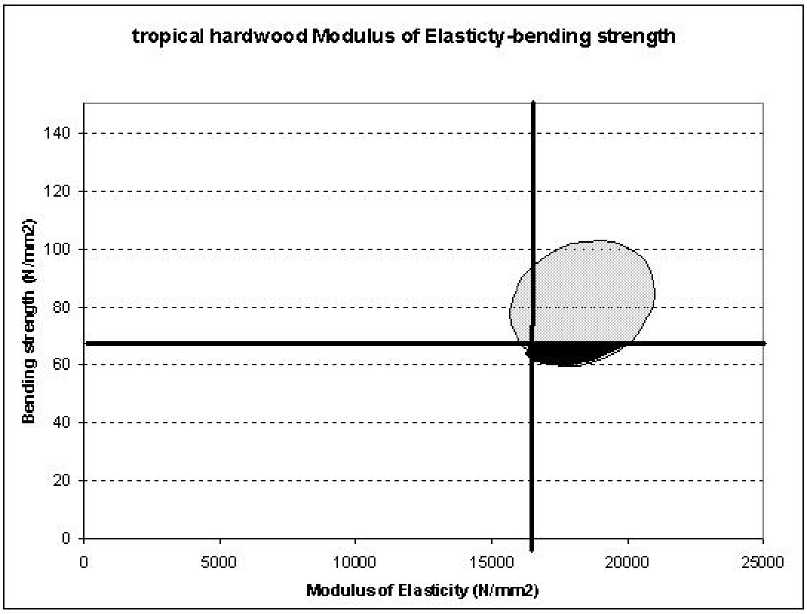

Figure 8: Typical correlation diagram for a hardwood species between Modulus of Elasticity and bending strength

Figure 8 shows that there is no profit in using the modulus of elasticity as a grading criterion since no more than one class can be distinguished. However, this is detected when hardwood species are observed on an individual basis. During this research the question arose if it is necessary to observe every hardwood species individually. Observing figures 7 and 8 it is not clear if a sample from each hardwood species is sufficiently representative to gain insight into the correlation of material properties with the bending strength. In this research project it is studied what the effect is on the prediction of the bending strength for individual hardwood species having little distinct visual characteristics, when the material properties of these species are regarded as coming from one population. The reason for this approach is that a wood species is defined only by its distinct botanical characteristics and the assumption is that judging the whole population of timber on material properties as knots, density and stiffness, will give better strength predictions to subpopulations or species-combinations.
To achieve the research goals, several testing programmes with many destructive and non-destructive tests were performed. Based on these data, formulas have been developed that can predict the characteristic timber strength given a small number of destructive tests. These models should describe the properties of the population to such a degree that the strength class of a new wood species can be determined with a sufficient level of reliability.

3.2 Test programme

The test programme covered a great number of wood species, for which the bending strength, modulus of elasticity and density were determined. The species were selected in such a way that the expected values of the material properties would cover the relevant range of values for timber. During several years a large number of wood species were tested [7], [8],[8],[10]. The wood species that were tested in these research programmes are listed in table 1. The goal for the separate research programmes was to determine the strength class of the tested wood species.
Besides the species mentioned in table 1 also a test sample of the species azobe was incorporated in the analysis part of the research. The species azobe (*lophira alata*) was already classified in a strength class in previous research. An overview regarding the mechanical properties of azobe has been described and accepted for publication [11]. Data out of softwood research on spruce, pine, douglas and larix, in which also non-destructive data was available, is used in the study to the correlation between part non-destructive and destructive measurements.

Table 1: Species that were tested in the research programme

Species	**Origin**	**Latin name**
Angelim vermelho	Brazil	*Dinizia excelsa*
Bangkirai	Indonesia	*Shorea leavis*
Basralocus	Surinam	*Dicorynia guianensis*
Cumaru	Brazil	*Dipteryx odorata*
Denya	Ghana	*Cylicodiscus gabunensis*
European oak	Poland	*Quercus robur*
European oak	Middle- and Central Europe	*Quercus robur*
Karri	South-Africa	*Eucalyptus diversicolor*
Massaranduba	Brazil	*Manilkara bidentata*
Nargusta	Bolivia	*Terminalia amazonia*
Piquia	Brazil	*Caryocar villosum*
Robinia	Hungary	*Robinia pseudoacacia*
Vitex	Solomon islands	*Vitex cofassus (spp)*

From all wood species, samples were taken with a minimum of 40 test pieces. The test pieces were beams with dimensions that are used in construction, for example 50 x 150 mm^2.
On every test piece the following data was established:

- Visual characteristics:
  a. Knots sizes
  b. Grain angle
  c. Other imperfections
- The mass of the test piece
- The moisture content measured with an electronic moisture meter.
- The moisture content derived with the oven dry method.
- The modulus of elasticity determined through measurement with the Mobile Timber Grader (dynamic modulus of elasticity E_{dyn})
- The modulus of elasticity determined through a 4-point-bending test according to EN 408 (static modulus of elasticity E_{stat})
- The bending strength determined through a destructive 4-point-bending test according to EN 408.

The test values were adjusted to the reference conditions according to European and Dutch standards [4], [6].

The test results have been processed for the following purposes:

- To determine the characteristic properties of the wood species according to EN 384 [3] and to classify the wood species into strength classes according to EN 338 [2].
- To investigate the correlations between non-destructive measurements and the standardized measurements according to EN 408 [4] for bending strength and modulus of elasticity.

The test results according to EN 408 are presented in table 2. The average bending strength, the coefficient of variation of the bending strength, the mean static modulus of elasticity and the mean density are given. All data has been adjusted to the reference conditions at a moisture content of 12%. In the last column the strength class according to EN 338 is presented. These strength classes are determined using the method described in EN 384, with the non-parametric method for the characteristic bending strength.
Species that could not be classified into a D-strength class for hardwood were classified into a C-strength class.

Table 2: Results of tests according to EN 384 and EN 408.

Species	**Mean bending strength (N/mm2)**	**Coefficient of variation of the bending strength**	**Mean Static modulus of elasticity (N/mm2)**	**Mean Density (kg/m3)**	**Strength class according to EN 338**
Angelim vermelho	82.9	0.21	16816	1045	D35
Bangkirai	96.3	0.23	20851	930	D50
Basralocus	70.5	0.33	21484	725	C22
Cumaru	115.5	0.21	20710	1017	D60
Denya	84.2	0.16	17727	947	D40
European oak, Polish	51.2	0.16	11596	616	C24
European oak, M+C. Europe	45.6	0.30	10358	684	C20
Karri	77.4	0.20	19302	706	D35
Massaranduba	124.5	0.14	24796	1034	D60
Nargusta	77.7	0.22	18349	723	C24
Piquia	76.6	0.22	21018	792	D35
Robinia	75.6	0.22	17704	699	D30
Vitex	69.8	0.19	16339	731	D30

3.3 Correlations between non-destructive measurements and standardized measurements according to EN 408.

3.31 General

The correlations between non-destructive measurements and the bending strength (and modulus of elasticity) according to the standardized methods of EN 408 were studied as a basis for the two research goals, mentioned in section 3.1. Therefore test results of the wood species are studied as an individual species being a population and as all wood species together being a population. This is discussed in the next sections.

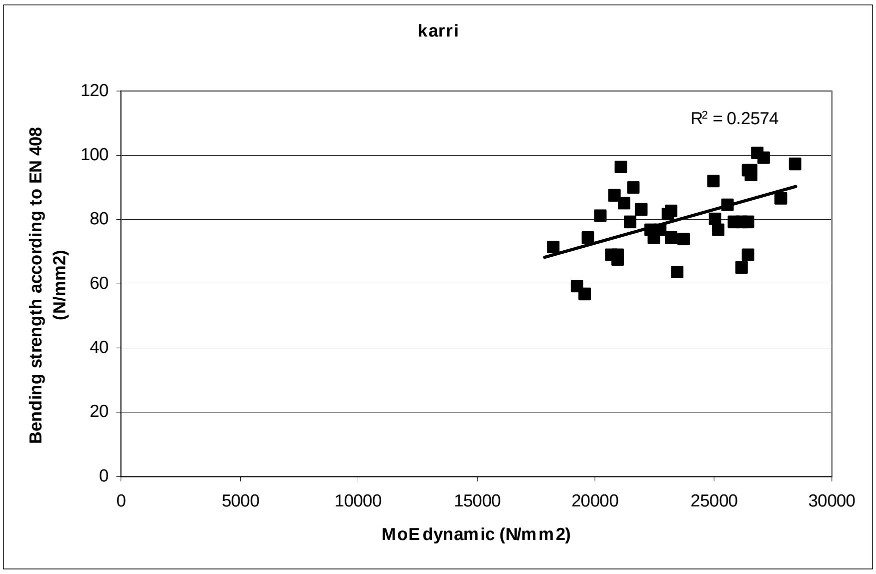

Figure 9: Test results of the species karri for the bending strength according to EN 408 plotted against the dynamic modulus of elasticity.

3.3.2 Predicting models based on test results of individual hardwood species.

According to the expectations formulated in section 3.1 the analysis showed that it is not possible to make reliable predicting models for all hardwood pieces individually, contrary to softwood species as pine and spruce. An example is given in figure 9 for the hardwood species Karri. What can be noticed is that the range of the bending strength values of this individual hardwood species does not start close to zero (this in contrast to softwood species, of which the minimum strength values for the bending strength are very close to zero). Furthermore the figure shows poor correlation between the Modulus of Elasticity and the bending strength.

A possible explanation could be that test samples from individual species do not have enough clear, distinct characteristics to be regarded as a specific subpopulation. The division in botanical species does not seem an appropriate way to determine strength predicting phenomena.

3.3.3 Prediction models based on test results regarding all hardwood species as one population.

When the hardwood species are not considered as individual populations, but are merged together to form one large population "timber", correlations between non-destructive measured properties and the bending strength appear to be good. This population has a sorting criterion that the beams (from all hardwood species) have restricted visual characteristics as knots. For now useful correlations between these properties and the bending strength can be found. These correlations apply to the entire range of values of the bending strength, from zero to the highest values, as shown in figure 10. Now the data of the species karri fit into the entire data set values of the population. So there is a prediction line that gives reliable predictions and can be used for optimisation.

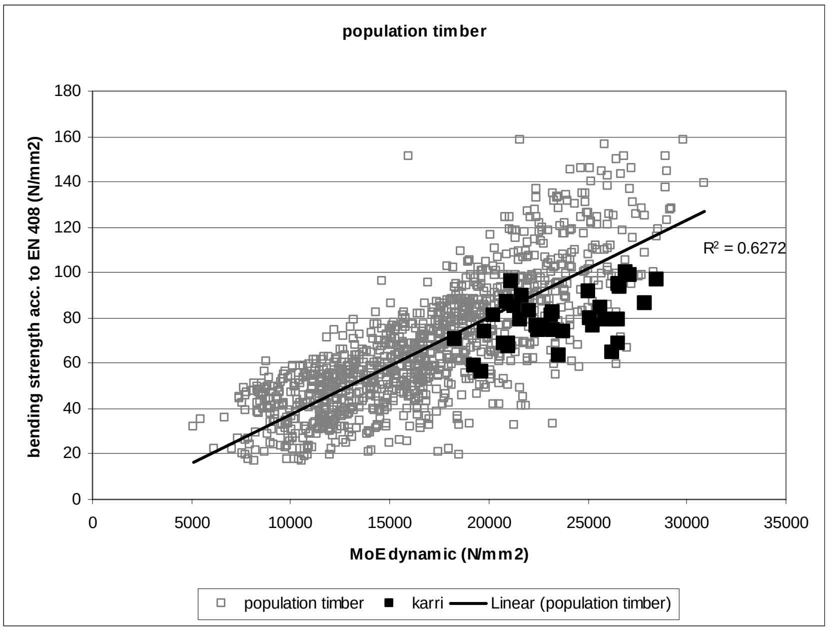

Figure 10: Test results for karri and for all species together of the destructive bending strength according to EN 408 plotted against the dynamic modulus of elasticity.

The main conclusion is that the bending strength of hardwood timber can be predicted for a specific wood species, when the behaviour of the material properties of the entire population of “timber” is taken into account. This opens the possibility to develop models for hardwood timber that can predict the bending strength of subpopulations as an individual species with the required reliability. With these predictions individual wood species can be classified into a strength class for visual grading in an economic way.

The best predicting model for the bending strength turns out to be a model where the predicting material properties are the dynamic modulus of elasticity and the density. A correlation coefficient r = 0,82 can then be achieved, as illustrated in figure 11.

In figure 12 is shown that the static modulus of elasticity has a strong correlation with the dynamic modulus of elasticity. For these properties a correlation coefficient of r = 0,85 was found.

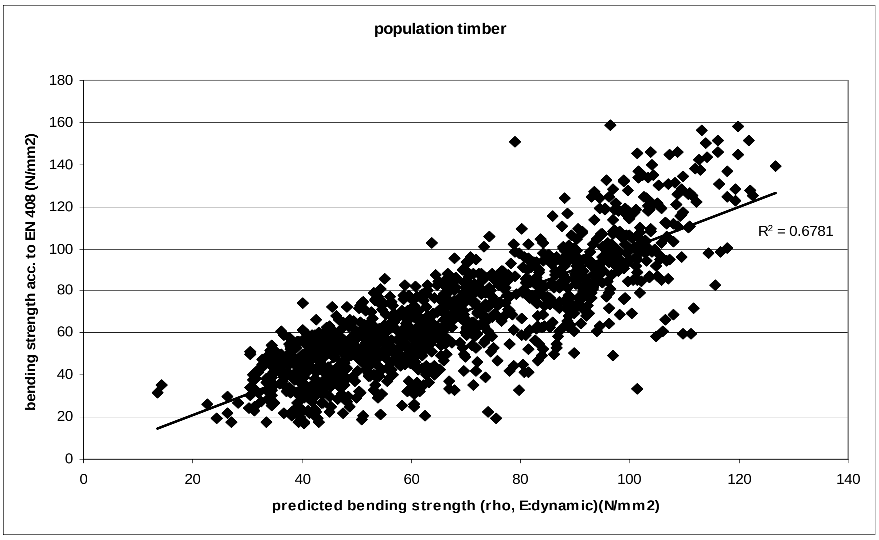

Figure 11: Test results of the bending strength according to EN 408 plotted against the predicted bending strength, using data of all species, based on a model with the density and the dynamic modulus of elasticity as predicting parameters.

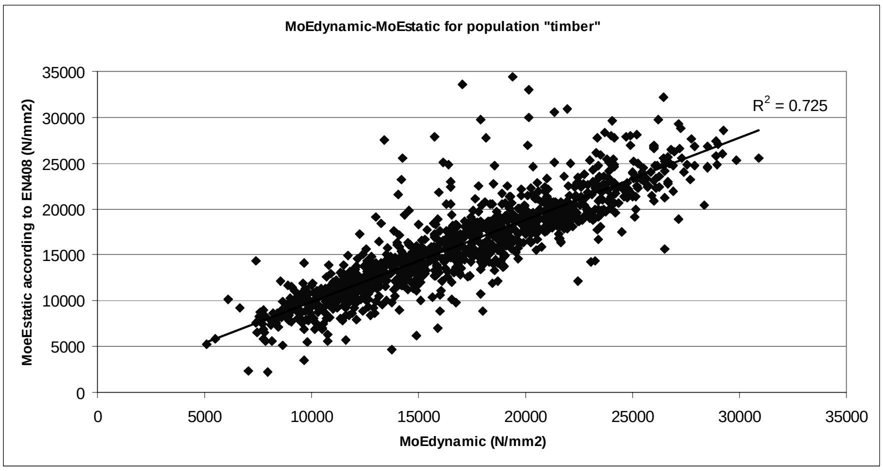

Figure 12: Test results of the static modulus of elasticity according to EN 408 plotted against the dynamic modulus of elasticity, using data of all species.

3.4 Analysing the distributions of the bending strengths of the tested wood species

3.4.1 The distributions of timber bending strength data.

As mentioned in section 2, traditionally non-parametric tests are used for determining the 5%-fractile strength value of wood species. However, according to Eurocode 1 parametric methods are preferred. But for timber, non-parametric tests are used as in that case knowing the actual statistical distribution and type of the test results is not necessary. The second reason is that by performing extensive tests (more than 300) it has been proven that a 5%-fractile of both the non-parametric distribution and the normal distribution is almost the same. For the classification of timber a minimum of 40 beams is allowed. For that reason the following questions were considered:

- Can the test values of the individual hardwood wood species be regarded as a sample from a normally distributed population? (see section 3.4.2)
- When the hardwood species are regarded as one population “timber”, do subsets generated with species-independent classification rules show normal behaviour? (see section 3.4.3)

If both assumptions are correct, the knowledge of the entire timber population can be used to classify a subset of this population by a parametric method.

3.4.2 Verification of the normal distribution of the test results of individual species

The distributions of the bending strengths of the tested wood species were investigated. It is often presumed that timber strength data can be described by a Weibull distribution. In [12] a large amount of softwood data sets were analysed and it was concluded that the normal distribution also gives a good description of the data for softwood. To verify this for hardwood all test data of individual species are considered to judge whether they can be seen as part of normal distributions [13]. Two plots of the data of all individual species are made. The first plot shows the normal probability of the dataset (when all data points are on the straight line the dataset is completely normal), as shown in figure 13a. Because the data is only a relatively small sample of a total population, it is possible that the sample is not quite normally distributed although the entire population is. To test if the sample is part of a normal distributed population a large number of samples are randomly taken from the normal distribution, represented by the straight line (Fig 13a). These are plotted together with the data of a specific species data set. This plot shows the range of datasets that can be expected when they are taken from a completely normal distribution. See figure 13 for the normal probability plot of the observed data of massaranduba (13a) and the range where the data is expected when they are taken from a population that is normally distributed (13b). This shows for the species massaranduba that the observed data could be a sample from a normal distributed population.

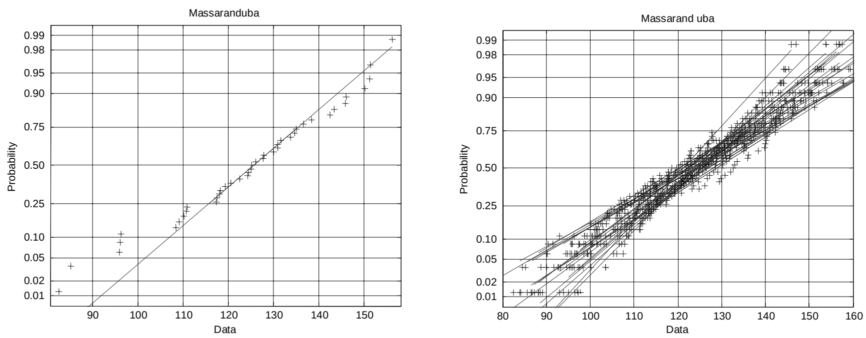

Figure 13: Normal probability plot of the test data of massaranduba (a) and a number of test samples from a normal distribution plotted together with the test data of massaranduba (b).

However, one restriction has to be made. For species with a lot of defects as knots and grain angle, a sample can fit on the normal distribution, but can have a deviation from the expected normal probability line that is not random (as for species with limited visual defects), but follows a pattern. When the sample is restricted on the visual defect that may occur, the sample fits better on the normal distribution. As an example the test data of Middle and Central European oak is plotted. In figure 14a no restrictions to the visual characteristics as knot sizes were made; all timber was considered to be useful for structural purposes, although in practice this is not true. Although this sample could be part of a normal distributed population, the deviation in the tail does not seem to be random, but has a systematic pattern. When restrictions are made to the knot sizes, see figure 14b, the test sample fits very well on the normal distribution and the deviations in the tail occur randomly.

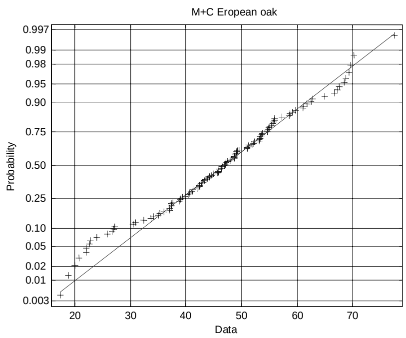

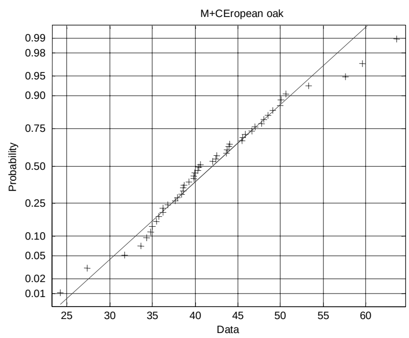

Figure 14: Normal probability plots of Middle and Central European oak with no restrictions to knot sizes (a) and with limited knot sizes (b).

The plots show that hardwood species can be considered to be normally distributed, when they are restricted to defects as knots and grain angle. In practice, these restrictions will be used to visually sort out the beams of a species, to which the determined strength class may be assigned. The beams that do not pass these restrictions should not be used for construction.

3.4.3 Normal behaviour of classified subsets of the entire population "timber"

In section 3.3.3 correlations are found between the bending strength and non-destructive measurements, when all species are regarded as belonging to one population "timber". These correlations can be used to make predictions. In chapter 4 these models will be explained. The bending strength of every beam, regardless the species, can be predicted with a certain safety level. Then, every beam can be classified in the D-classes available from D35 to D70. Because the beams are classified with a certain safety level that is both reliable (only 5% is allowed to be incorrectly upgraded) and economic (which depends on the accuracy of the model), many of the actual values derived by destructive tests, will be higher. However, the distribution of these actual values that are predicted to be in the same D-class, can be analysed. In figure 15a a probability plot for normal behaviour of the beams classified to be in strength class D40 is shown and in figure 15b the same for strength class D60.

Figures 15a and 15b show normal behaviour. This means that when the entire set of hardwood data is regarded as one population “timber”, models can be formulated which can classify the population into subsets that are normally distributed.

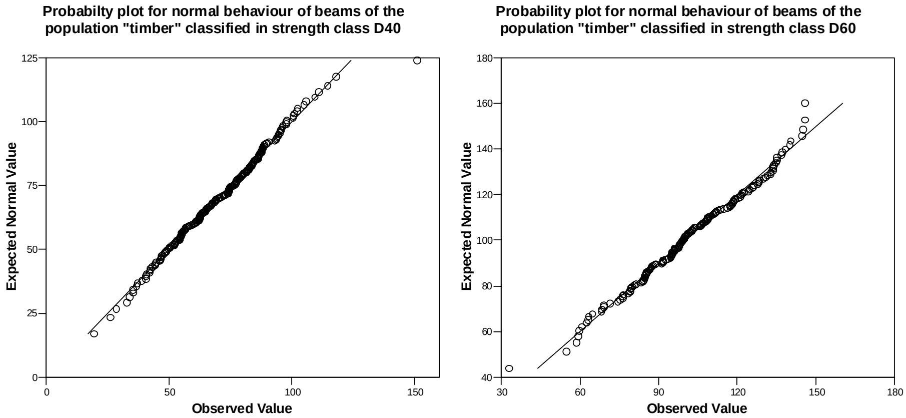

Figure 15: Normal probability plot for the actual values of beams of the population “timber “ that are classified to strength class D40 (a) and D60 (b) with predicting models.

3.5 Conclusions

In section 3.3 correlations have been found between non-destructive measurements on the one hand and the standardized destructive bending strength and the standardized modulus of elasticity on the other. As a result accurate economic predicting models can be made to classify hardwood timber in different strength classes.

Section 3.4 describes that datasets of hardwood species can be regarded as subsets from a normal distribution. When hardwood timber is regarded as one population “timber”, this population can be classified in subsets that show normal behaviour.

An economic method using combined destructive and non-destructive measurements can be developed with these findings. This method makes use of a parametric distribution (the normal distribution) to classify “new” wood species into a strength class. This method is described in section 4.

4 Classification of new wood species with combined destructive and non-destructive tests

4.1 General

In section 3.3 general correlations between material properties independent of the wood species were found. Section 3.4 displays that the normal distribution gives a good description of the bending strength of wood species. Combining these two facts makes it possible to classify new hardwood species in an economic way. When new species are regarded as a subpopulation of the entire timber population, for which we know general properties, it is possible to classify new wood species with a smaller number of destructive tests. In this chapter a model is presented that can predict the 5%-fractile bending strength for a wood species on the basis of combined destructive and non-destructive tests. The basic principle of this method is the following: 75% of the beams will be tested non-destructively and 25% will be tested destructively according to EN 408. So, for the minimum sample size of 40 beams this means 10 destructive tests and 30 non-destructive tests. With this method the 5%-fractile can also be calculated for other ratios of destructive and non-destructive measurements.

The non-destructive measurements are related to:

- Dimensions of the timber beam
- Weight, measured with a balance
- Moisture content, measured with a moisture meter
- Dynamic modulus of elasticity, measured with the TNO Mobile Timber Grader

For 75% of the beams, the bending strength of the beams will be calculated on the basis of the predicting regression lines.

The measurements according to EN 408 are:

- Moisture content with the oven dry method
- Static modulus of elasticity, measured with a bending machine
- Bending strength

In sections 4.2 and 4.5 the models for the bending strength and the modulus of elasticity are described. The methods to calculate the 5%-fractile bending strength and the mean Modulus of Elasticity using the non-destructive and destructive measurements are described in sections 4.4 and 4.6.

4.2 The correlation between non-destructive measured material properties and the bending strength for the population "timber".

A general bending strength model has to be formulated that correlates the bending strength according to EN 408 with the material properties that are measured non-destructively. This model is based on analysis of the non-destructive and destructive test results of all beams in the research programme. All test data are adjusted to the reference moisture content of 12%.
For the bending strength the following model was formulated:

$$f_b = g(\rho, Edyn) + \varepsilon \qquad (1)$$

where

f_b is the model bending strength (N/mm^2).

$g(\rho, E_{dyn})$ is the bending strength regression line with ρ and E_{dyn} as input parameters (N/mm^2).

ρ is the density (kg/m^3).

E_{dyn} is the dynamic modulus of elasticity measured with the Mobile Timber Grader (N/mm^2).

ε is the uncertainty in the prediction model.

$g(\rho, E_{dyn})$ can be a linear, but also a non-linear model. The lineair model is given by:

$$g(\rho, E_{dyn}) = a\rho + bE_{dyn} + c \tag{2}$$

where

$g(\rho, E_{dyn})$ is the predicted bending strength (N/mm^2)

a,b and c are constants.

The distributions of ρ, E_{dyn} and ε are supposed to be normal.

The uncertainty in the prediction model ε is stochastic with $\mu(\varepsilon) = 0$, $\sigma(\varepsilon) = \sigma_\varepsilon$. Investigation of the test results showed that the value of σ_ε varies with the value of $g(\rho, E_{dyn})$. The larger $g(\rho, E_{dyn})$, the larger σ_ε, see the dotted lines in figure 16.

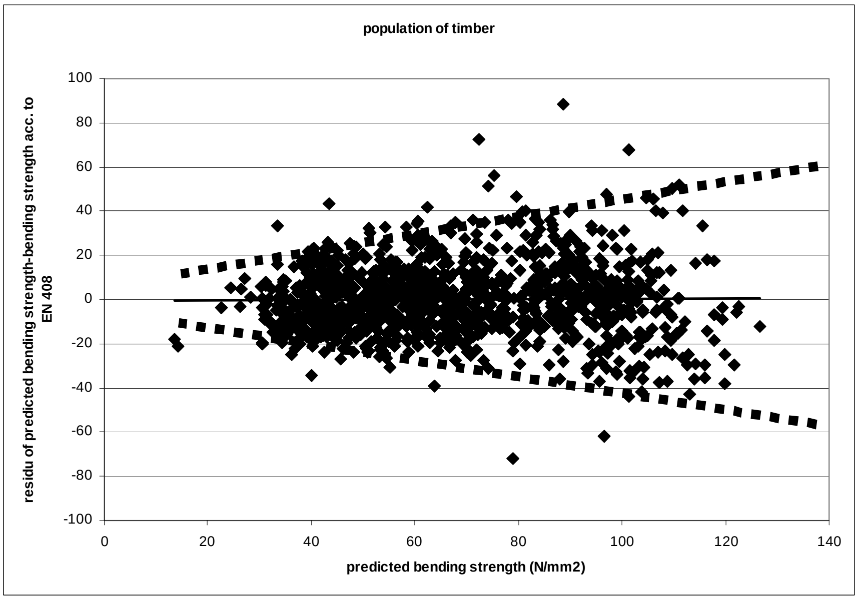

Figure 16: The model standard deviation increases with bigger values of the predicted bending strength

The relation between the predicted value of the bending strength and the value of σ_ε is linear and can be described in the following way:

$$\sigma_i(\varepsilon) = d * g_i(\rho, E_{dyn}) \qquad (3)$$

where

$\sigma_i(\varepsilon)$ is the value of $\sigma(\varepsilon)$ in point $g_i(\rho, E_{dyn})$ (N / mm²).

$g_i(\rho, E_{dyn})$ is the predicted value of the bending strength (N / mm²).

d is a constant.

4.3 Calculation method for the 5%-fractile of the bending strength with a computer model based on Bayesian statistics.

The 5%-fractile of the bending strength can now be calculated. For this purpose a computer model based on Bayesian statistics has been developed, which incorporates both destructive and non-destructive measurements. The backgrounds for this computer model will be outlined in a future publication. In the next paragraph a hand calculation method is presented. This method is presented because it is easy to use and gives a good insight into the various uncertainties.

4.4 A hand calculation method to find the 5%-fractile of the bending strength from combined destructive and non-destructive test results.

The 5-fractile of the test samples is calculated with the following equation:

$$f_{0,05} = \mu(f_{i,j}) - 1,64 * \sigma(f_{i,j}) \qquad (4)$$

In (5) $\mu(f_{i,j})$ and $\sigma(f_{i,j})$ are:

$$\mu(f_{i,j}) = (\mu(g_i) * n_i + \mu(g_{des\,;j}) * n_j) \;/\; (n_i + n_j) \qquad (5)$$

$$\sigma(f_{i,j}) = \sqrt{\;(\sigma(g_{des\,;j})^2 + \sigma_{\mu(g_i)}(\varepsilon\,)^2)} \qquad (6)$$

where

$\mu(f_{i,j})$ is the average value for the sample of the combined predicted and destructively measured bending strengths (N / mm²).

$\mu(g_i)$ is the average value of the bending strengths predicted by non-destructive measurements (N / mm²).

n_i is the number of beams on which non-destructive measurements are performed.

$\mu(g_{des;j})$ is the average value of the bending strength, measured by destructive measurements (N / mm²).

n_j is the number of beams on which destructive measurements are performed

The proportion between n_i and n_j is n_i / $n_j = 3$ and the minimum for $n_i + n_j = 40$.

$\sigma(f_{i,j})$ is the resulting standard deviation

$\sigma(g_{des;j})$ is the standard deviation of the destructive measurements (N / mm²).

$\sigma_{\mu(g_i)}(\varepsilon)$ is the model uncertainty according to equation (3) in point $\mu(g_i)$ (N / mm²), multiplied by the factor n_i / $(n_i + n_j)$: $\sigma_{\mu(g_i)}(\varepsilon) = \sigma_i(\varepsilon) * n_i \,/\, (n_i + n_j)$

4.5 The correlation between non-destructive measured material properties and the static modulus of elasticity for the population "timber".

A number of models for the static modulus of elasticity have been considered. The linear model has the best fit:

$$E_{stat} = e\, E_{dyn} + f + \varepsilon \qquad (7)$$

where

E_{stat} is the predicted value of the modulus of elasticity (N / mm²).

e and f are constants

ε is the uncertainty of the model, which is a stochastic with $\mu(\varepsilon) = 0$, $\sigma(\varepsilon) = \sigma_\varepsilon$.

The value of σ_ε is constant for the modulus of elasticity, regardless its value.

4.6 A hand calculation method for the 50%-fractile of the modulus of elasticity.

The characteristic value of the modulus of elasticity is equal to the mean value.
The 50%-fractile can be calculated with the following equation.

$$E_{0,50} = \mu(E_{i\,j}) - 0{,}2 * \sigma(E_{i,j}) \qquad (8)$$

In (9) $\mu(E_{i\,j})$ and $\sigma(E_{i,j})$ are given by:

$$\mu(E_{i\,j}) = (\mu(E_i) * n_i + \mu(E_{stat\,;j}) * n_j) \,/\, (n_i + n_j) \qquad (9)$$

$$\sigma(E_{i,j}) = \sqrt{(\sigma(E_{stat;j})^2 + \sigma_\varepsilon^2)} \qquad (10)$$

where

$\mu(E_{i\,j})$ is the average value of the sample of the combined predicted values out of the dynamic modulus of elasticity and the measured modulo of elasticity by static bending tests (N / mm²).

$\mu(E_i)$ is the average value of the modulus of elasticity predicted by the measurements of the dynamic modulus of elasticity (N / mm²).

n_i is the number of beams from which the dynamic modulus of elasticity was measured

$\mu(E_{stat;j})$ is the average value of the modulus of elasticity of beams measured by static bending tests (N / mm²).

n_j is the number of beams from which the modulus of elasticity was measured by static bending tests.

The proportion between n_i and n_j is $n_i / n_j = 3$ and the minimum for $n_i + n_j = 40$.

$\sigma(E_{i,j})$ is the resulting standard deviation of the modulus of elasticity.

$\sigma(E_{stat,j})$ is the standard deviation of the modulus of elasticity measured by static bending tests (N / mm^2).

σ_ε is the model uncertainty (N / mm^2), multiplied by the factor $n_i / (n_i + n_j)$: $\sigma_\varepsilon = \sigma_\varepsilon * n_i / (n_i + n_j)$.

5 Comparison with test results

5.1 General

In this section the 5%-fractiles for the bending strength and the mean values for the modulus of elasticity, calculated out of the test results for all beams according to EN 408, will be compared with the values calculated from the combined destructive and non-destructive tests according to the presented new method of section 4.

5.2 The 5%-fractile of the bending strength

In figure 17 the 5%-fractiles for the bending strength according to the non-parametric method calculated using the standardized measurements according to EN 408 are compared with the values according to the presented model in section 4 based on combined destructive and non-destructive tests. In figure 18 the ratios of these two values are presented. The average ratio is 1,07. This is above 1, which is slightly conservative but low enough to give beneficial results.

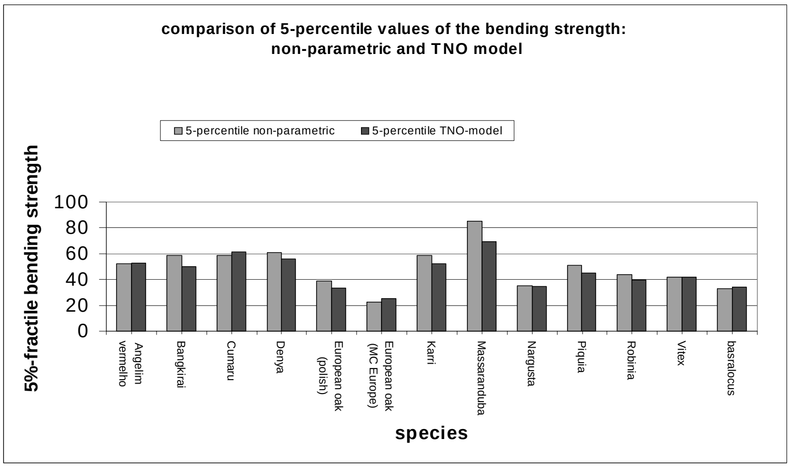

Figure 17: Comparison of 5%-fractile bending strength values determined with the non-parametric method and calculated with the TNO model.

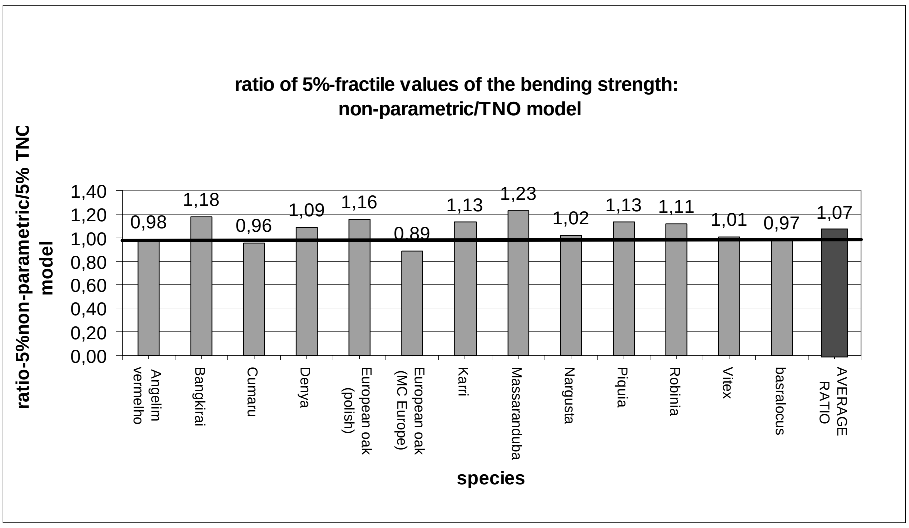

Figure 18: Ratio's of the 5%-fractile bending strength values for the non-parametric method divided by the value calculated with the TNO model

5.3 The mean modulus of elasticity

In figure 19 the mean values for the modulus of elasticity, in accordance with the standardized testing methods according to EN 408, and the modulus of elasticity determined by the presented model of chapter 4 based on combined measurements, are compared. The average value of the ratios is 1,06, which is above 1. This is slightly conservative, but low enough to give beneficial results.

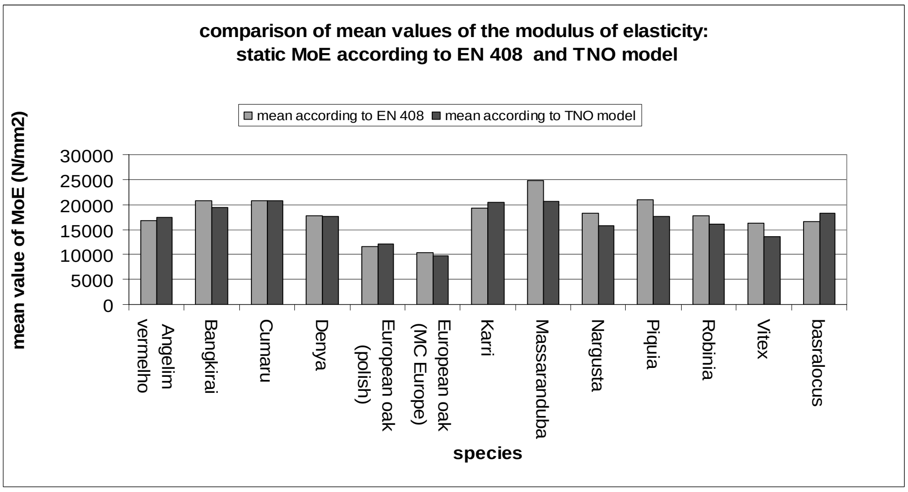

Figure 19: Comparison of the mean values of the modulus of elasticity determined with the static modulus of elasticity according to EN 408 and the modulus of elasticity calculated with the TNO model.

5.4 Conclusions

The verification shows that the presented models for the bending strength and modulus of elasticity correlate good with the traditional method. They are slightly conservative compared to the traditional method for the test samples.

Considering the use of the traditional non-parametric method a remark has to be made: for different test samples coming from the same population there can be significant differences for the 5%-fractiles of the bending strength.

The presented models are based on parametric methods, which create the possibility to take the expected variability between different test samples into account. It can be concluded that the presented methods are a good alternative for the traditional standardized methods.

6 Application of the new method for the classification of new wood species.

In 2003 a project was performed with the classification of 9 new wood species in a strength class using the new method in commission of FSC Netherlands. An overview of the final results is presented in table 3.

Table 3: Strength classes of 9 new wood species, determined using the presented model

Species	Latin name	Origin	Strength class according to EN 338, derived by the new model
Cupiuba	Goupia glabra	Brazil	D35
Louro itauba (itauba)	Mezilaurus itauba	Brazil	D40
Sucupira amarelo	Qualea paraensis D..	Brazil	D40
Sucupira vermelho	Andira spp	Brazil	D30
Uchi torrado (Uxi)	Sacoglottis guianensis, Vantanea parviflora, V. micrantha	Brazil	D40
Muiracatiara (Gonçalo-Alvez)	Astronium graveolens Jacq., A. fraxinifolium Schott, A. lecointei Ducke, A. Urundeuva	Brazil	D40
Jarana	Lecythis spp	Brazil	D40
Sapucaia	Lecythis pisonis	Brazil	D50
Piquia marfim	Aspidospermum desmanthum	Brazil	D50

In table 4 the derivation of the characteristic values of the bending strength and the modulus of elasticity of the test sample are presented for the species Sapucaia. They are calculated according the calculation models of section 4.4 and 4.6. See these sections for the explanation of the symbols.

Table 4: Derivation of the characteristic values of the bending strength and the modulus of elasticity of the test sample of sapucaia.

Derivation of the characteristic value of the bending strength of the test sample of sapucaia according section 4. 4. All values in N/mm² **(n_i / n_j = 3)**		**Derivation of the characteristic value of the modulus of elasticity of the test sample of sapucaia according to section 4.6.** **All values in N/mm²** **(n_i / n_j = 3)**	
$\mu(g_i)$	105,8	$\mu(E_i)$	22568
$\sigma_i(\varepsilon)$	23,3	$\sigma(\varepsilon)$	3550
$\sigma_{\mu(g_i)}(\varepsilon)$	17,5	σ_ε	2662
$\mu(g_{des;j})$	106,7	$\mu(E_{stat;j})$	25892
$\sigma(g_{des;j})$	12,5	$\sigma(E_{stat,j})$	4154
$\mu(f_{i,j})$	106,0	$\mu(E_{i\,j})$	23400
$\sigma(f_{i,j})$	21,5	$\sigma(E_{stat,j})$	4934
$f_{0,05}$	70,6	$E_{0,50}$	22412

The characteristic bending strength of the test sample is 70,6 N / mm². Because there were 40 specimens in the test sample, this value has been reduced with a sample factor of 0,78 according to [3] to a value representative for the population of the species sapucaia. This value of 0,78 * 70,6 = 55,1 N / mm² has been compared with the values of the strength class system of EN 338 [2]. Since this value is higher than 50 N / mm² the strength class that could be assigned to the species sapucaia is D50. The characteristic values for the modulus of elasticity and the density of the test sample were also higher than those of strength class D50 of EN 338 [2].
The strength classes mentioned in table 3 are used in compliance with the requirements for visual grading that are stated in the Dutch guidelines for timber in waterworks.

7 Future developments for machine grading

In this paper it has been explained that for most hardwood species, when using visual inspections, only one visual grade can be distinguished. When the beams do not meet the requirements of the visual characteristics, they cannot be used in construction. However, the research has shown that when grading is not done visually but by mechanically measured properties, such as the dynamic modulus of elasticity, weight and moisture content, it is possible to grade beams of a hardwood species into more than one strength class. To accomplish this TNO has developed the Mobile Timber Grader.

Figure 20: Lab prototype of the Mobile Timber Grader. Beams of different wood species and different sizes can be graded.

In this research the Mobile Timber Grader was used for the determination of the dynamic modulus of elasticity. The device has also been equipped with a software tool for predicting the strength class. The device does not only fill up the gap between expensive in-line grading machines and visual grading, it also makes machine grading possible for beams that cannot be graded by in-line machines, see figure 21

Figure 21. The Mobile Timber Grader makes it possible to machine grade beams of large sizes.

8 Conclusions

A new method to classify new hardwood species has been presented. When this method is used, less destructive bending tests are necessary, compared to traditional methods. The research shows strong correlations between properties predicted from non-destructive measurements on the one hand and the bending strength and the modulus of elasticity derived according to standardized tests on the other. To make these correlations visible all wood species are regarded as belonging to one (super) population. A computer calculation model to determine the 5%-fractile of the bending strength has been developed, together with a hand calculation model. This hand model was verified with the test data from standardized tests. The results are reliable and also very economical, since their values are slightly conservative compared to the traditional method as a reference. For the mean value of the modulus of elasticity also a hand calculation model has been developed.
Applying the method the visual characteristics, such as knots and grain angle, have to be restricted. These restrictions are being used to visually grade the beams.

References

[1] prEN 14081-1 Timber Structures – Strength graded structural timber with rectangular cross section- part 1 : General requirements

[2] EN 338. Structural Timber – Strength classes, 2003

[3] EN 384, Structural timber – Determination of Characteristic values of mechanical properties and density

[4] EN 408, Timber structures – Structural timber and glued laminated timber – Determination of some physical and mechanical properties

[5] Goerlacher, Sortierung von Brettschichtholzlamellen nach DIN 4074 duch Messung von Longitudinalschwingungnen. Bauingenieur vol. 65,1990

[6] NEN 6760, TGB 1990 Timbers structures, 2002

[7] Van de Kuilen, J-W.G., Ravenshorst, G.J.P. Bending strength and stress wave grading of (tropical) hardwoods, COST E24 Zurich, 2002

[8] Van de Kuilen, J-W.G. Development of a general determination method for the strength of timber. Phase 1. TNO Reports 1999-LBC-R7027 / R7028/2 / R7029 / R7030/2. (in Dutch)

[9] Van der Linden, M.L.R., Van de Kuilen, J-W.G., Blass, H.J., Application of the Hoffman Yield Criterion for load sharing in timber sheet pile walls. Pacific Timber Engineering Conference pp. 1994

[10] Van de Kuilen, J-W.G., Ravenshorst, G.J.P. Development of a general determination method for the strength of timber Phase 2. TNO Reports 2000-CHT-R101 / R102 / R156 / R157 /R158 / R172 / R173 / R174 / R178 / R179 (in Dutch).

[11] Van de Kuilen, J-W.G., Blass, H.J. Mechanical properties of azobe (lophira alata), Holz als Roh-und Werkstoff . DOI 10.1007/s00107-004-0533-7.,2005.

[12] Sorensen,J.D. and Hoffmeyer, P.,Statistical Analysis of Data for Timber Strengths, Aalborg University, 2001

[13] De Wit, S. and van de Wiel, W., Characteristic timber strength of a timber sample, TNO paper, 2004.

Potential wood protection strategies using physiological requirements of wood degrading fungi

Michael Sailer and Bas van Etten

TNO Building and Construction Research, Delft, The Netherlands

Due to the increasing restrictions in the use of wood preserving biocides a number of potential biocide free wood preserving alternatives are currently assessed. Wood degrading fungi require certain conditions in the wood in order to be able to use wood as a food source. This paper discusses the physiological requirements of wood degrading fungi and potential wood protecting strategies based on the limitation of essential requirements of the fungi. Most of these methods are based on reduction of the water and nutrient availability, two factors which can by influenced by the application of some preservation techniques.

Key words: wood, wood degradation, non- biocidal wood preserving strategies

1 Introduction

Wood is a multi-use biological raw material with a high economic importance for a number of industrial sectors such as construction, furniture and the packaging industry. However, its natural durability performance is critical for cost-effective performance over the whole life of a building or construction component and is much more variable than that of materials such as concrete or metal. Under unfavourable conditions, fungal or insect activity or other detrimental impacts, the service life of some wood products can be limited.

In order to overcome the susceptibility of wooden products for wood degrading organisms, wood species with a high durability or biocidal wood preservative treatments are used. The environmental acceptance of many wood preservatives however is very low at present. The EU legislation is restricting the continued use of CCA preservatives and creosote. It is however evident that the importance of wood in the building sector is related to the service life of products made of wood or wooden products.

The question arises which potential non-biocidal alternatives can be applied and at least partly replace the substances that will probably only be used to a small extent in future. In this paper potential non-biocidal developments and methods in wood preservation are discussed.

2 The physiological basis for wood degrading fungi

The activity of micro-organisms and therefore also wood degrading fungi is depending on a number of physical, chemical and biological factors.
The occurrence and ratio of these factors can act as a stimulator or hinder their activity until a complete stop of growth. These factors are therefore considered as important elements in the non biocidal prevention of the degradation activity of wood degrading fungi. The knowledge and use of these factors in order to influence the fungal growth is one of the keys in wood conservation.
Four main points have been identified that offer the potential to influence the fungal activity:

- Wood moisture
- Nutrients
- Oxygen
- Temperature

An optimum of these 4 aspects can lead to high fungal activity. If only one of these factors can be changed in a way that it does not fulfil the fungal requirements, degradation should be limited.

2.1 Wood moisture

The water availability for fungi is influencing the degradation processes to a large extent and is therefore the most important factor in wood conservation. The fungi need water in order to take up the nutrients and for transport processes within the mycelium (Table 1). The enzymes, which are required for wood degradatation, are depending on water and the hyphea of fungi are also consisting of 90% water (Schmidt 1994).
The water occurs in wood as hygroscopic water or as bound water. The hygroscopic water or capillary water is found in liquid form in the lumina and other cavities in the wood, whereas the bound water is located in the cell wall and bound to the hydroxyl groups of the celluloses, hemicelluloses or lignin.
The moisture content of materials is often expressed as the percentage of moisture based on the dry mass of the material.

u [%] = ((mw-md)/ md) x 100
u = moisture content
m = mass of wood wet
md = mass of wood dry

Table 1: Range of moisture contents for typical wood degrading fungi (Schmidt 1994):

	Minimum moisture content [%]	**Optimum moisture content [%]**	**Maximum moisture content [%]**
Coniophora puteana (Brown rot)	24- 30	30-70	60-80
Serpula lacrymans (Brown rot)	17-30	30-60	55-90
Coriolus versicolor (White rot)	25-30	35-55	60-90

The micro-organisms however can not use the whole water of the substrate but only the water that is not bound by dissolved substances such as salts, sugars etc.. Finally is not the absolute moisture content the essential factor on fungal activity, but the wateractivity, which is invluenced by matrix potential and pores (Table 2) of the materials. They determine to what extent the water can be used by the micro-organisms. The water activity (a_w) is defined as the ratio between the water vapour pressure of the solution (p_S) and the water vapour pressure of pure water (p_W) (Schmidt 1994, Carlile *et al* 1995).

$$a_w = p_S / p_W$$

Table 2: Water availability in different environments

Water activity	**Water potential**	**Pore radius µm**	**Examples**
1.0	0		Celllumina, pure water
0.9993	-0.1	1.5	Fibre saturation
0.98	-2.8	0.5	Sea water
0.97	-4.2	0.035	Lower limit wood destroying fungi
0.96	-5.6	0.026	Leaf litter
0.90	-14.5	0.01	Ham
0.80	-30		Low limit for Aspergillus and
0.60	-69		Penicillium
			Limit for cell-growth

In order to overcome dry periods the fungi can produce dry resistant mycelium or spores. The mycelia of some basidiomycetes are considered as dry resistant. In tests it was found out that under favourable conditions the mycelium of fungi like *Coniophora puteana* or *Gloeopyllum abietinum* can keep their growth ability for several years.

In most cases however is the forming of dry resistant spores for fungi the most efficient strategy to overcome critical climate conditions.

2.2 Temperature

The temperature is also influencing the fungal activity. In most cases wood degrading fungi cannot be active at temperatures below 0°C. At lower temperatures the water is frozen and the enzymes cannot be active due to lack of liquid water. The temperature optimum depending on the fungus is between 20-40°C, with a maximum of 50°C. At temperatures of more than 50°C the degradation of the proteins is the limiting factor, restricting the synthesis of enzymes. In practise however it is very difficult to influence the temperature of the surrounding of wooden buildings, the application of the higher temperatures to protect the wood is therefore practically limited to remedial treatments.

2.3 Oxygen

Although the reduction of oxygen offers a certain protection potential the method depends in practice on a very high water content in the wood and its surroundings in order to replace the oxygen in the wood. Examples are wooden poles in areas with high ground water and the wood storage under water. The exclusion of oxygen is very much dependent on the surrounding and can therefore not easily be controlled.

2.4 Nutrients

The main components of the world's biomass, polysaccharides and lignin can be degraded by a large number of micro-organisms. Wood consists mainly out of polysaccharides such as hemicelluloses and celluloses (Table 3) and is therefore a potential food source for wood destroying fungi.

Table 3: Proportion of main wood components

	Softwood [%]	**Hardwood [%]**
Cellulose	42-49	42-51
Hemicelluloses	24-30	27-40
Lignin	25-30	18-24
Extractives	2-9	1-10

The different wood components are degraded by the enzyme systems of the fungi and are distinguished according to the degradation patterns. The three main rot types are:

- Brown rot
- White rot
- Soft rot

The degradation patterns are formed by specialized microorganisms with specific enzyme systems. The efficiency of these enzymes to attack wood is depending on several factors:

- Contact with the substrate
- Moisture content
- Interactions with the substrate

The degradation of the wood requires penetration of the enzymes into the cell walls of wood (Figure 1). A number of wood degrading enzymes have been identified, most of them are however too big to penetrate through the micro pores of the wooden cell wall (Kirk 1985).

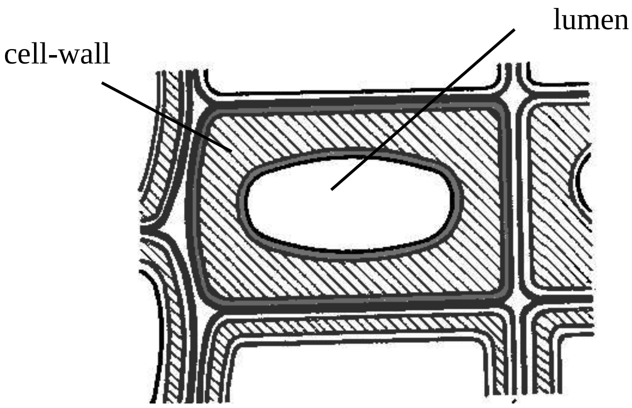

Figure 1: Cell-wall of a typical softwood

How the relative large enzymes manage to penetrate the wood is not yet clear. Most of the pores in the wooden cell wall have a diameter between 2 and 4 nanometer (nm) (Kirk 1985, Rapp 1999, Hale *et al.* 2003) and are therefore too small for most of the enzymes (Table 4).

Table 4: Size of different enzymes

Enzymes	**Size**
Cellulases	5.0 nm spherical or 3.3 x 20 nm if ellipsoidal
Xylanase	7 nm
Lignin peroxidases	4.7 nm (spherical) of 4.3 nm x 6.0 nm

Obviously also some other systems are effective. The penetration of different low molecular wood degrading substances (LMWDAs) is suggested as a possible initial degrading mechanism.

The white rot morphology is characterized by the removal of celluloses and in a later stage the degradation of celluloses. White rot enzymes (peroxidases, laccases and others) are too large for initial cell wall penetration. The LMWDA's play probably an important role especially in lignin degradation.
For the brown rot fungi (*G. trabeum*) a chelator mediated Fenton system (CMFS) is suggested, using Fe, ortho dihydroxy catechol, H_2O_2 and hydroxyl radicals (Hale *et al.* 2003).

Non-biocidal wood protection strategies

Based on the physiological requirements of the fungi some potential non-biocidal wood protection strategies are regarded. The main targets are in most cases the moisture and nutrition requirements. Changes in the wood shall restrict the conditions that are required for wood degradation. Principally two different treatments are distinguished: Treatments which do not cause changes within the cell wall and treatments that cause changes within the wooden cell wall. Treatments that cause changes on cell wall level are also known as wood modification. Examples of potential wood treatments are presented in Figure 2.

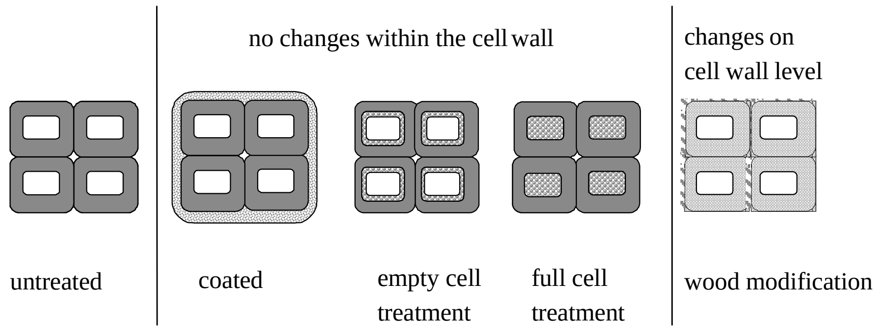

Figure 2: Examples of different potential wood treatments

3.1 Treatments without changes in the call wall

Exceeding a certain moisture content over a period of time is considered as one of the main degradation factors. A wood moisture content of more than 20%-25% is considered as critical and can cause wood rot. The most frequent non-biocidal wood preservation strategy used is therefore the reduction of moisture content. In wood expositions without permanent ground contact is the application of hydrophobic substances on the wood surface a commonly applied method.
Intact coatings possess a strong water repellent effect. A typical character of surface treatments on wood is however the reduced efficiency caused by ageing processes at exposition (Sell 1980**,** Nilsson 1993). At a low vapour permeability of the coatings the water content is often increased

within the wood after water penetration through cracks or damages in the coating. This leads to a increased risk of fungal decay (e.g. Sell 1973, Williams 1991).

Because of the non-biocidal efficiency of hydrophobing coatings within the wood and the low surface protection of not film forming impregnations new combination processes have been assessed. The combination of coatings and impregnations with bioeffective substances was tested by a number of researchers (e.g. Evans *et al.* 1992, Williams and Feist 1999**,** Breyne 1999). Also impregnations with hydrophobic resins have been suggested (Peek *et al.* 1992, Sailer *et al.* 1998, Passalis and Voulgaridis 1999). The hydrophobation effect of oil-treatments at Scots pine is demonstrated in Figure 3.

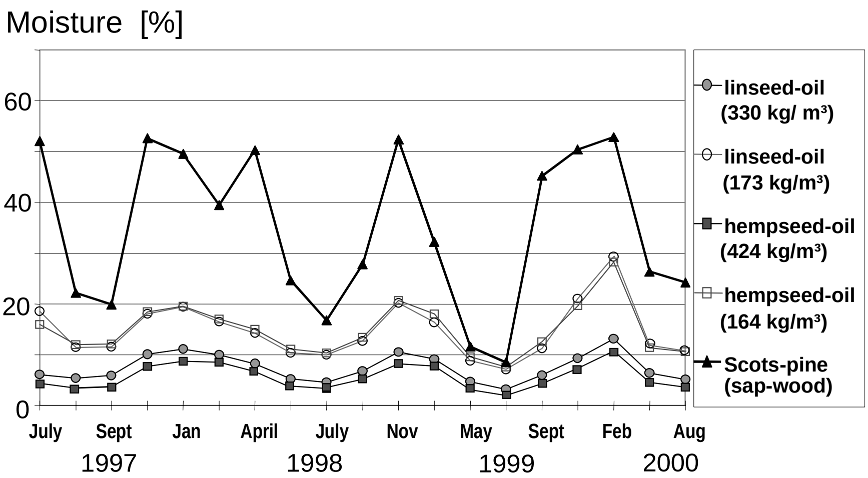

Figure 3: Moisture contents of treated and untreated Scots pine at outdoor exposition

The hydrophobing effect of a filmforming oil-impregnation which is observerd at outdoor exposition can be attributed to the combination of different factors:

1. Intact coatings as received with high oil-loadings and temperature treatment possess a strong water repellent effect.
2. At high retentions of oils is the wateruptake of liquid water via the capillaries delayed (Dirks 1999). The periods with higher moisture contents are in practice very often too short for wood degrading fungi at expositions without ground contact. A high moisture content will be however achieved in permanent ground contact or sourrounding with a high moisture content over a longer period.

3.2 *Changes on cell wall level*

Enzymes, especially the polysaccharides are very substrate specific. According to Kirk (1985) almost any synthetic modification of the substrate will prevent effective contact with the modification site of the substrate polymer. The most assessed treatment that claims to substitute the hydroxyl groups of the cellulose or hemicelluloses is the acetylation. Other potential wood modification processes are based on the impregnation of the wooden cell wall with substances such as silicates (Figure 4), furfuryl alcohol, melamine resins or the application of higher temperatures, which degrades the wood structure to a certain content (Figure 5).

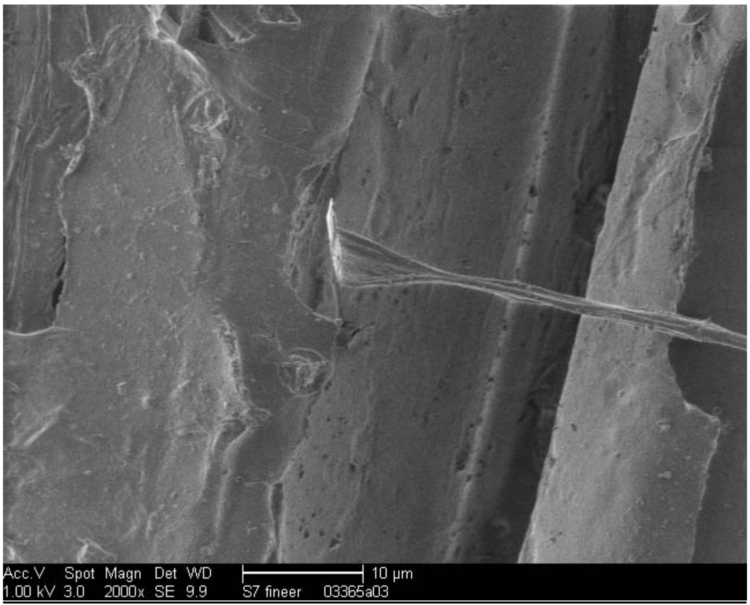

Figure 4: With silanes treated Pinus sylvestris after exposition to the brown rot fungus Coniophora puteana.

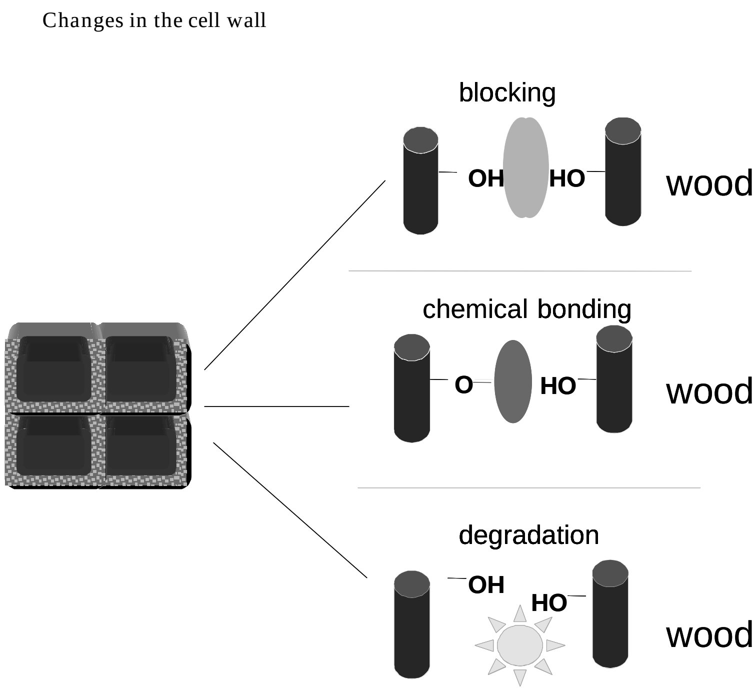

Figure 5: Possible changes in the wooden cell wall with effects on the wood properties

3.3 Combination treatments

Few authors only assessed the combination of modifications of the wood on cell-wall level and an additional hydrophobation by lumen filling substances. Rowell *et al*. (1982) treated pine and marple with propylenoxid-triethylamin and impregnated the wood later with methyl-metacrylat (MMA), Hafizoglu and Yildiz (1990) impregnated acetylated wood with linseed-oil and Sailer *et al.* (2000) combined the heat-treatment of wood with vegetable oils and achieved a good performance of the treated wood in durability tests according to the European standard EN 113. A combination treatment of acetylation and impregnation with melamine resins that resulted in a good durability in sea water is described by Epmeier *et al.* 2003.

3.4 Mode of effectiveness

Since the modification of the wood substance reduces the moisture content in the wooden cell wall (Rapp1999) it is not clear whether decay resistance is due to a hindering of enzyme action or disruption of necessary water relations (Kirk 1985). New research however suggests that the blocking of the space in the cell wall might be one of the effective mechanisms at treatments of wood with different substances (Lukowsky 1999, Hill and Hale 2004). That however implies that the efficiency of wood modification is not necessarily based on chemical changes of the wood substrate but also on the limitation of the accessibility of the wooden cell wall.

References

Breyne, S. 1999: >>Royal<< Schutzverfahren erfolgreich optimiert". Holz-Zentralblatt 70, 1029

Carlile, M. J.; Watkinson, S. C. 1995: The fungi. Academic press, London, 482 S.

Dirks, H. 1999: Anwendungsmöglichkeit von vegetabilen Ölen zum Feuchteschutz von Holz. Diplomarbeit Universität Hamburg, 160 pp

Epmeier,H , Westin, M. Rapp, A. O. and Nilsson, T. 2003: Comparison of Properties of Wood modified by 8 different Methods –Durability, Mechanical and Physical Properties. In Proceedings of the First European Conference of Wood Modification, Ghent 2003

Evans, P. D.; Michell, A. J.; Schmalzl, K. J. 1992: Studies of the degradation and protection of wood surfaces.. Wood Sci. Technol. 26, 151-163

Fritsche, W 1999: Mikrobiologie. Spektrum, Akad. Verl. Heidelberg, Berlin, 622 pp

Hale, M. D., Hill, C. A. S. Farahani, M. R., 2003: Decay of Silane Modified Wood, Proceedings of the COST E 22 meeting in Zagreb.

Hill C.A.S.; Hale, M. 2004: Investigations of the role of cell wall moisture content and microporeblocking in the decay protection mechanism of anhydride modified wood. Final Workshop COST Action E22 'Environmental Optimisation of Wood Protection' Lisboa – Portugal, 22nd - 23rd March 2004

Hafizo lu, H.; Yildiz, Ü. C. 1990: Acetylation plus water-repellent treatment of wood in slate thickness. Holzforschung 44: 245-248

Kirk T. K. 1985 The chemistry and biochemistry of decay. In: Wood deterioration and its prevention by preservative treatments, volume 1, Degradation and Proctection of wood.

Lukowsky, D. 1999: Holzschutz mit Melaminharzen. Dissertation, Universität Hamburg, 194 pp

Nilsson, K. 1993: Träskyddsbehandlingar (Wood protection treatments). Swedish Wood Preservation Institute Nr. 168, 74pp

Passialis, C. P.; VoulgaridisS, E. V. 1999: Water Repellent Efficiency of organic solvent extractives from pine leaves and bark applied to wood. Holzforschung 53, 151-155

Peek, R.-D.; Militz, H.; Kettenis, J. J. 1992: Improvement of some technological and biological properties of poplar wood by impregnation with aqueous macromolecular compounds. IRG / WP 92-3721, 20

Rapp, A. O. 1999: Physikalische und biologische Vergütung von Vollholz durch Imprägnierung mit wasserverdünnbaren Harzen. Dissertation, Universität Hamburg, 230 pp

Rowell, R. M.; Moisuk, R.; Meyer, J. A. 1982: Wood-polymer composites : Cell wall grafting with alkylene oxides and lumen treatments with methyl methacrylate. Wood science 15 (2), 90-96

Sailer, M. 1998: Biological resistance of wood treated with waterbased resins resins and drying oil in a mini-block test.. IRG / WP 98-40107, 10

Sailer, M.; Rapp, A. O.; Leithoff, H.; Peek, R.-D. 2000: Vergütung von Holz durch Anwendung einer Öl-Hitzebehandlung. Holz als Roh- und Werkstoff 58: 15-22

Schmidt, O. 1994: Holz- und Baumpilze. Biologie, Schäden, Schutz, Nutzen. Springer-Verlag, Berlin, 246 pp

Sell, J. 1973: Über den Einfluß von Oberflächenbehandlungen auf Pilzschäden an Holz-Außenbauteilen. Schweizerische Arbeitsgemeinschaft Holzforschung 1: 3-8, 16

Sell, J. 1980: Oberflächenbehandlung von Brettschichtträgern. Holz-Zentralblatt 40 / 41, 629; 630

Williams, R. S. 1991: Effect of acidic deposition on painted wood. . J. Coat. Technol. 63, 53-73

Williams, R. S.; Feist, W. C. 1999: Water repellents and water-repellent preservatives for wood. Forest Products laboratory. General Technical report FPL-GTR-109, USDA Forest Service Forest Products laboratory Madison WI 53705-2398, 12 pp.

Surface temperature of wooden window frames under influence of solar radiation

C.J.J. Castenmiller

TNO Building and Construction, Delft, The Netherlands

Under influence of solar radiation the surface temperature of wooden window frames can reach values above 60 ^{0}C. High temperature can cause considerable tensions within the window frame; as a result joints can be cracked and rain water can penetrate into these joints. This penetration of rain water is often the start of considerable degradation of the window frame. Which surface temperatures can be reached depends on the colour of used paint and the orientation of the surface. The frame sill appears to be the surface that is most heated by solar radiation; window frames that are painted in a dark colour show the highest surface temperatures because of the relatively high absorption coefficient of dark coloured paints. Calculations with an dynamic model are made to predict which surface temperature can be reached on sunny days. It appears that surface temperatures up to more than 60 ^{0}C can be reached. To avoid these high surface temperatures light coloured paints are preferable.

Key words: sun radiation, surface temperature, wooden window frames

1 Introduction

From experience it is known that the total solar radiation on a surface depends on its orientation. Horizontal surface receive normally more radiation than vertical surfaces. Shadowing from others constructions parts or buildings will however reduce the total received solar radiation. The more radiation a surface receives the higher the surface temperature can rise. Furthermore the colour of the surface plays an important roll; dark coloured surfaces reaches higher surface temperatures then light coloured surfaces.
Which surface temperature can be reached on a sunny day is calculated with a dynamic model; in such model the heat capacity of the material is taken into account. The heat capacity is defined as the amount of heat (energy) that is needed to change the temperature of 1 kg material 1 degree Celsius (or Kelvin) and is expressed in J/(kg.K).

2 Solar radiation

The flux density of solar radiation on a surface normal to the sun's rays and beyond the earth's atmosphere is not constant but varies during the year. As the earth's orbit is not perfect circular but slightly elliptical and the solar radiation intensity varies inversely as the square of the sun-earth distance the maximum intensity is reached in mid-winter (for the northern hemisphere), when the earth is closest to the sun. The minimum intensity is reached in mid-summer and is about 7 % lower then the maximum value.
Furthermore the earth's axis is tilted at an angle of 23.5 degree to its orbital plane, therefore the solar declination also varies during the year (see figure 1)

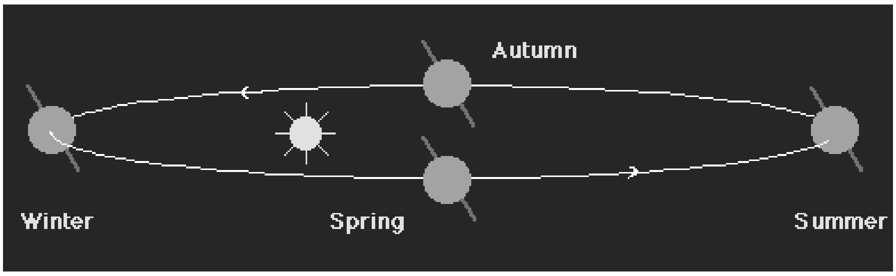

Figure 1: Solar declination during the year

At the 21st of March and September the declination is 0 degree; at the 21st of June the declination is 23,5 degree; at the 21st of December the declination is –23.5 degree.
In figure 2 the solar declination is given during a year; the days are number from 1 (1st of January) till 365 (31st of December).

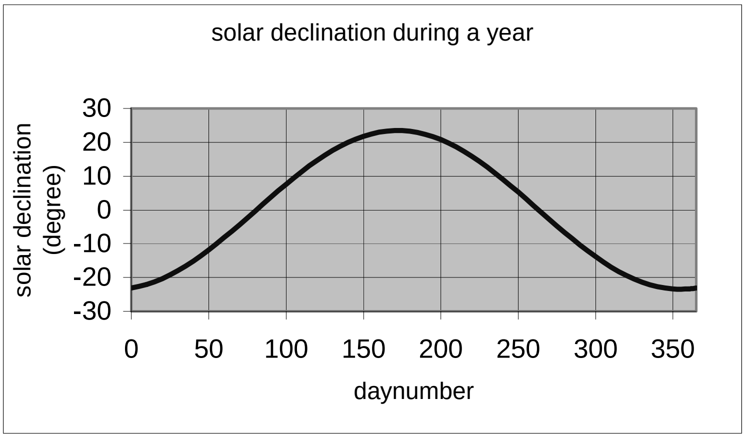

Figure 2: Solar declination during a year

As a result the flux density on a certain place on earth varies; this variation causes the changing of seasons and the unequal periods of daylight.
A surface can receive solar radiation directly radiated by the sun. However, passing through the earth's atmosphere the sun's radiation is scattered and absorbed by water vapour, ozon, dust and gas molecules. Some of the short wave radiation which is scattered reaches the earth in the form of diffuse radiation. Since this diffuse radiation comes from all parts of the sky its intensity is difficult to predict and is subject to a wide variation due to moisture and dust content. This is however the reason why surfaces facing (a part of) the sky can receive solar radiation, although the surface is not direct radiated by the sun. Besides direct and diffuse radiation a surface can receive radiation due to reflection from the ground or for instance buildings.
The direct solar radiation on a surface depends on the sun's position in the sky and the orientation of the surface. The solar position depends on the latitude L, the solar declination (δ) and the time. The solar position can be characterised by the solar altitude (or elevation) and the solar azimuth (see figure 3).

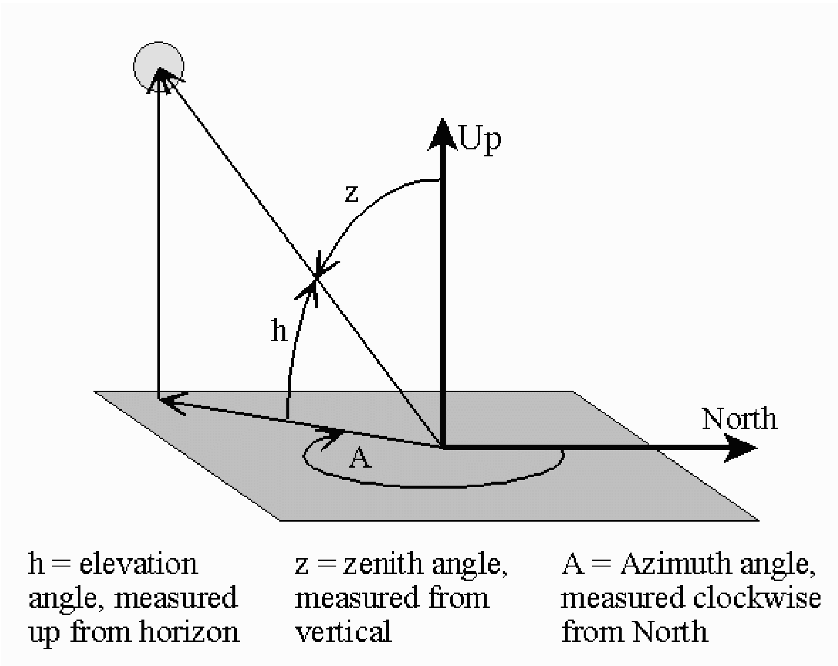

Figure 3: Position of the sun in the sky

The solar altitude (h) above the horizon and the solar azimuth (A_z) can be calculated by:

$$\text{Sin}(h) = \cos(L)\cos(\delta)\cos(t) + \sin(L)\sin(\delta) \quad (1)$$

$$\sin(A_z) = \cos(\delta)\sin(t) / \cos(h) \quad (2)$$

Where t is the hour angle, measured in relation to the south direction. The hour angle can be calculated by:

$$t = 15.(Ts-12) \quad (3)$$

where Ts = solar time .

Solar time is 12 o'clock when the sun reaches his highest position during that day. If differs form clock time due to the latitude, the date and the time zone. The difference between clock time and solar time can amount to about 50 minutes (+ 1 hour in the summer).

The incident angle on a surface (I) is related to the solar altitude (h), the surface-solar azimuth (A_{ss}) and the orientation of the surface (E = the angle of the surface from horizontal) by:

$$\cos(I) = \cos(h)\cos(A_{ss})\sin(E) + \sin(h)\cos(E) \quad (4)$$

The value of the direct normal solar intensity (I_{dn}) – measured perpendicular on the direction of the sun rays - on the earth on a clear day varies during the year because of seasonal changes in the dust and water vapour content of the atmosphere and also because of the changing of the earth-sun distance.

The average value of I_{dn} during the year is given in figure 4 (see [1]). For very clear atmospheres (for instance in mountainous areas) the value of I_{dn} can be as much as 20 % higher; in very dirty atmospheres (industrial area) the value of I_{dn} can be as much as 20 % lower.

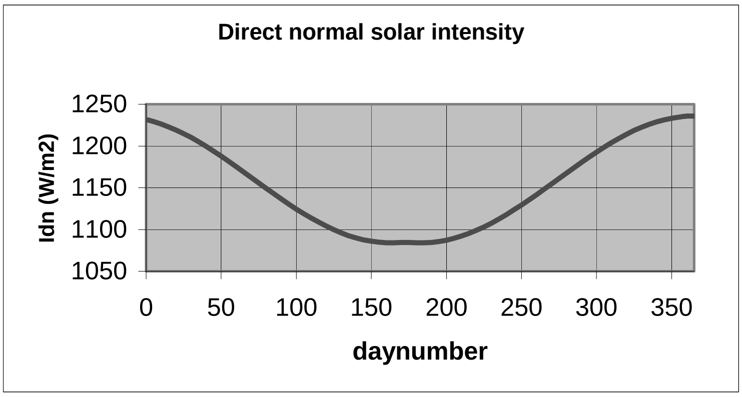

Figure 4 Direct normal solar intensity during the year

The diffuse solar radiation (I_{ds}) (see [1]) can be calculated approximately by the equation:

$$I_{ds} = C.I_{dn}.Fss \quad (5)$$

Where Fss is the angle factor between the surface and the sky. The value of C varies, like the value of I_{dn}, during the year; the values are derived from [1] and is given as a function of the day number in figure 5.

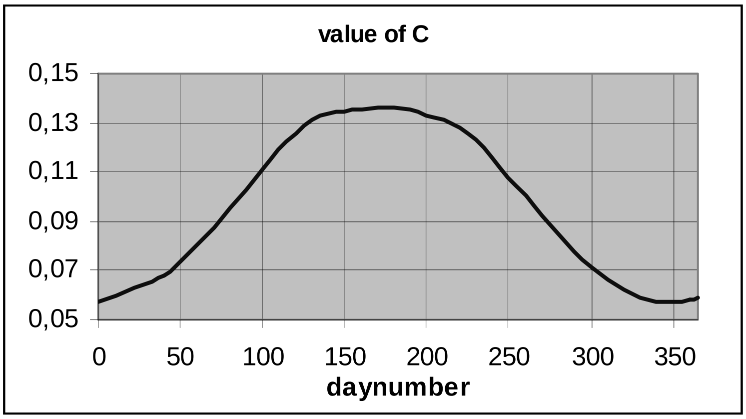

Figure 5: Value of C during the year

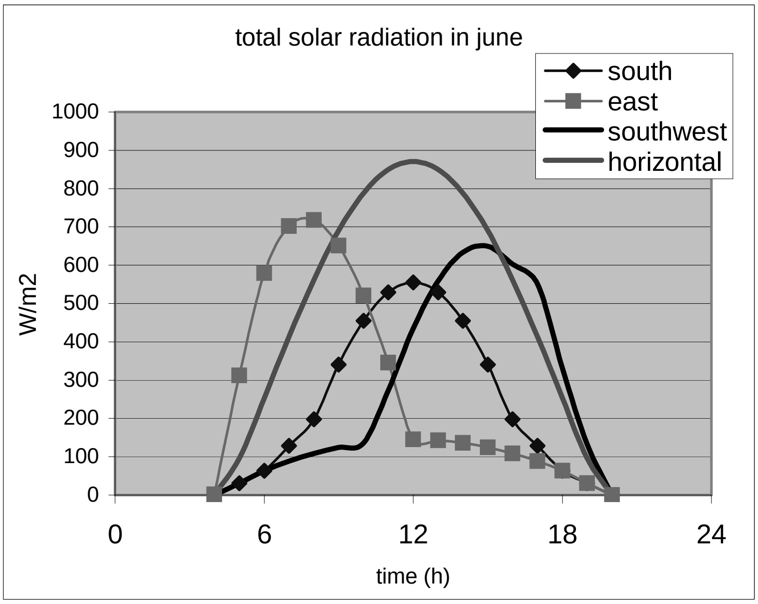

Figure 6: Total solar radiation in June for surfaces with different orientation

3 Solar radiation on a surface

The solar radiation on a surface depends on the orientation of the surface. A vertical surface facing east will receive direct solar radiation at sunrise, while a vertical surface facing west only receives direct radiation after noon (when the sun passes its zenith). A horizontal surface can receive solar radiation during the whole day when no shadowing from the surrounding area (like other buildings or constructions) appears. The total solar radiation (direct and diffuse) for different orientations is given in figure 6 for the month of June.
As can be seen in figure 6 a horizontal surface will receive the most radiation on a sunny day. A east facing (and also a west facing) vertical surface receive more radiation than a south facing vertical surface.
As a result the highest surface temperatures can be expected for horizontal surfaces.

4 Calculation of the surface temperature

The temperature a surface reaches under the influence of solar radiation is dependent not only on the total solar radiation but also on the air velocity at the surface and on the absorption coefficient of the surface. During a day the surface temperature normally increases due to the solar radiation and will therefore be higher than the surrounding air temperature.
Heat exchange with surrounding air increases with increasing air velocity at the surface. The highest surface temperatures can therefore be expected at calm, windless weather conditions.
The heat exchange between the surface and the surrounding air can be characterised by the surface coefficient of heat exchange or the α-value. Normally an α-value of 20 W / (m^2.K) for free convection (heat exchange due to differences in temperature between surface and surrounding air) is used.
The amount of solar radiation absorbed by a surface depends on the absorption coefficient of the surface; because wooden window frames are mostly painted the absorption of solar radiation depends on the absorption coefficient of the paint (a).
The absorbed total solar radiation can be calculated by:

$$I_{tot} = a \cdot (I_{dn} + I_{ds}).\cos(I) \qquad (6)$$

Dark paints have a higher absorption coefficient then light coloured paint. In table 1 some absorption coefficient are given for different coloured paints.

Table 1: The absorption coefficient for solar radiation for some paints

Colour of the paint	**Absorption coefficient**
White	0.25
Crème	0.35
Light yellow	0.45
Light green	0.50
Grey	0.75
Black	0.97

4.1 The increase of the surface temperature

For a standard used timber window frame in the Netherlands the increase of the surface temperature due to solar radiation is calculated. Theses calculations are made with a dynamic program; heat capacity of the material is taken into account.

The air temperature on the inside and the outside of the window frame is considered to be equal and constant, so the calculated increase of the surface temperature is fully the result of the solar radiation.

As an example the increase of the surface temperature for the frame sill of a window frame with east orientation is given in figure 6. For the absorption coefficient of the surface the value 1 (maximum possible value) is used.

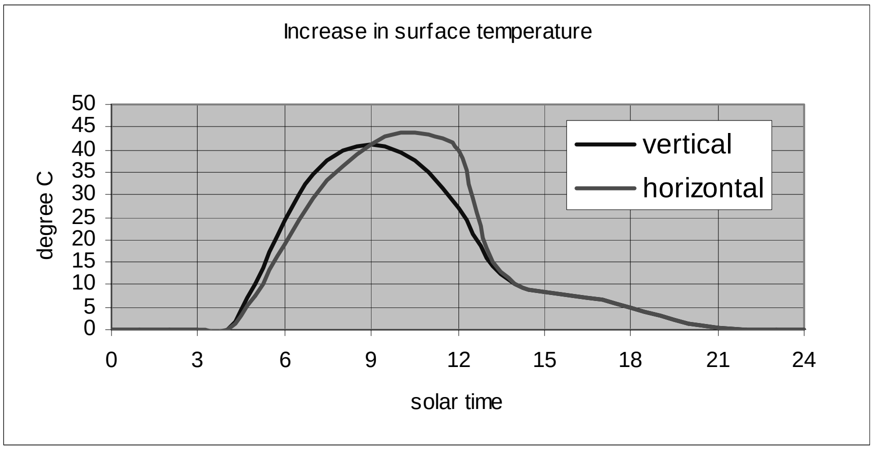

Figure 7: Increase of the surface temperature during a sunny day in June for an east orientated window frame

It is important to know that the time is given as solar time; this means that the sun reaches his highest altitude at12 o'clock'. The clock time in the Netherlands is about 40 minutes behind and in the summer even 1.40 hour behind.
As can be seen in figure 6 the surface temperature of the vertical front side increases more rapidly than for the horizontal side due to the fact that a vertical surface receives more radiation early in the morning. As the sun rises the incident angle on a vertical surface decreases where the incident angle on a horizontal surface increases. Eventually the surface temperature of a horizontal surface reaches higher values then on a vertical surface. Maximum is reached at about 10 o'clock.
A second example is given in figure 7; here the surface temperature is given for a vertical intermediate post with a south orientation.

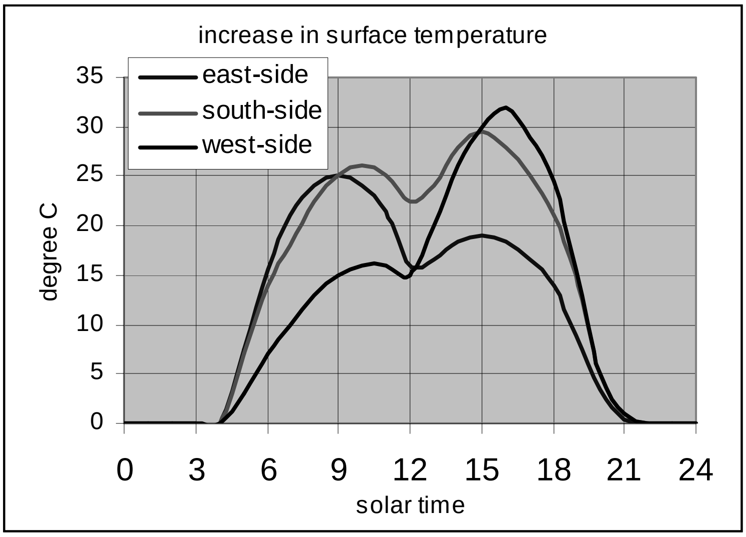

Figure 8: Increase in surface temperature for a sunny day in June for a vertical intermediate post

This figure shows a more complicated picture. The surface temperature on the east side of the vertical post rises more quickly as this part is radiated first. After about 9 o'clock the surface temperature drops but increases again after 12 o'clock influenced by the surface temperature on the front and the west side of the post. The surface temperature on the front side of the post decreases after about 10 o'clock because the incident angle on this surface decreases and the surface receives less radiation. In the afternoon the incident angle increases again and the surface temperature rises again, also under the influence of the surface temperature on the west side.

The surface temperature at the west side increases in the morning due to the surface temperature on the east side and the front; after 12 o'clock the west side receives direct solar radiation and increases more rapidly.

5 Maximum surface temperatures

The maximum increase of surface temperature is calculated for both sills and posts as an function of the orientation and the absorption coefficient of the surface (paint).
The results are given in table 2.

Table 2: Maximum increase of surface temperature (in degree Celsius) due to solar radiation

Absorption coefficient of the used paint	**Frame sill (horizontal surface)**		
	East in June	South in March	Southwest in June
0.6	26.0	24.3	28.1
0.7	30.7	31.8	32.8
0.8	35.0	36.4	37.5
0.9	39.4	40.9	42.2
1.0	43.8	45.5	46.9
	Intermediate vertical post		
	East in March	South in June	Southwest in August
0.6	19.4	18.2	19.3
0.7	22.6	21.2	22.6
0.8	25.8	24.0	25.8
0.9	29.0	26.9	29.0
1.0	32.3	29.8	32.2
	Side post orientated on the South, in June		
0.6		17.8	
0.7		20.8	
0.8		23.7	
0.9		26.7	
1.0		29.7	

Actual surface temperature can be obtained by adding the increase of the surface temperature due to solar radiation (table 2) to the outside air temperature. For the outside air temperature the maximum outside air temperature can be used.

In table 3 the maximum outside air temperature during the period 1998 – 2003 is given for the Netherlands for March till September.

Table 3: Maximum outside air temperature for the Netherlands in the period 1998-2003

	1998	**1999**	**2000**	**2001**	**2002**	**2003**
March	19.3	19.3	15.8	13.2	14.5	19.5
April	21.7	20.8	23.0	22.2	20.4	24.7
May	32.0	28.1	29.6	25.3	25.5	27.5
June	29.7	25.3	33.6	28.6	23.7	28.1
July	30.5	30.6	24.9	31.6	31.0	34.3
August	30.9	31.4	28.9	31.4	29.5	35.0
September	22.5	29.3	23.9	19.2	23.1	24.9

6 Conclusions

Table 2 shows the increase of the surface temperature which can reach values up to 45 ^{0}C above air temperature. From table 3 it is clear that air temperatures more than 30 ^{0}C are possible. Therefore surface temperature of dark coloured painted window frames can reach values of more than 75 ^{0}C. Such high temperatures can cause high tension inside the window frame and joints can be cracked. Penetration of rain water inside these joints can start degradation of the window frame.

Temperatures up to 60 ^{0}C must be avoided to limit these risks. This can be reached by applying light coloured paints.

References

[1] ASHRAE: Handbook of fundamentals, American Society of Heating, Refrigerating and Air-Conditioning Engineers, Inc., New York (1968)

[2] Recknagel-Sprenger: Taschenbuch fur Heizung + Klimatechnik, R.Oldenburg Verlag GmbH, Munchen, Wien (1979)

[3] CRC Handbook of chemistry and physics, Edition 78th, 1997-1998

Heat treated wood and the influence on the impact bending strength

A. J.M. Leijten

Delft University of Technology, Delft, The Netherlands

As part of a national research program for the development of a timber guardrail tests have been conducted to gain knowledge about the impact strength of timber. Tests were carried out on Angelim Vermelho, Douglas Fir, Ash and Larch and three temperature treated wood species, Douglas Fir, Spruce and Pine. Three point impact bending tests were performed with a loading speed of 7m/s. A high-speed camera was used to determine the time of failure. Computer simulations were used to determine the bending moment at the time of failure as literature showed other methods to be inadequate or questionable. Peculiar impulse transmitting effects were detected by the high-speed camera (9000 images/s). It was concluded that the impact strength is wood species and grade dependent. Some wood species didn't show any significant bending strength reduction for others the strength reduction was dramatic.

Keywords: guardrail, timber, impact, crash barrier, wood species, strength

1 Introduction

The starting point for the determination of many engineering timber properties is the standard short duration test where failure is expected within a few minutes. However, there are a number of load cases such as earthquakes and single blasts where timber is exposed to substantially higher loading rate.

In a number of countries, Netherlands and the USA, timber guard-rail systems are being considered as alternatives for the traditional steel guard-rail or concrete barriers. Old test data shows that timber is well able to withstand impact loads. However, the validity of the old test data is questioned as more elaborate recent research indicates conflicting results. For the Dutch guard-rail project a test programme was set up and carried out to gain more knowledge about the impact strength of structural wood. This paper summarises former test data and reports the test and computer simulation results of the experiments that were carried out within the framework of this guard-rail project.

2 Literature review of impact strength of timber

Historically, impact-bending tests were the first types of impact tests. Bodig et.al. [1] mentions the Hatt-Turner test, characterised by the application of impact loads in succession during the early 1900s. During the Second World War, when wood was used to a considerable extent for structural members for training aircraft's and gliders, it became evident that additional test data were necessary to improve the understanding of the behaviour of wood under impact load.

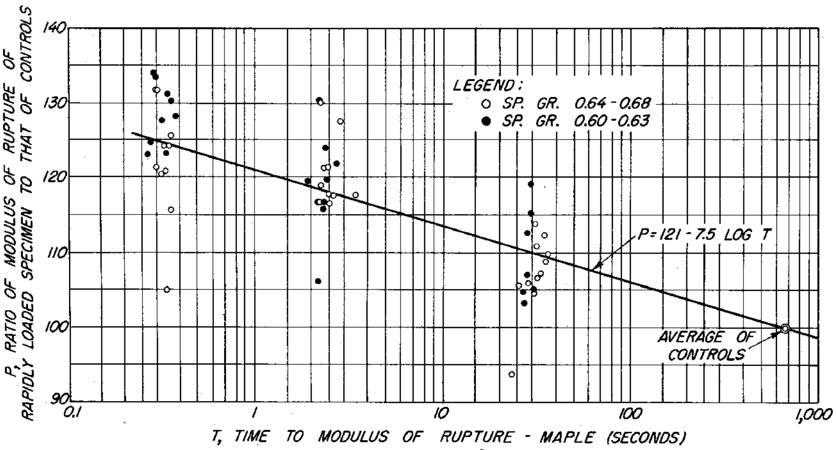

Figure 1: Ratio of static and impact bending strength versus loading rate for Maple, Liska [2].

Therefore, a comprehensive test program was initiated at the Forest Products Laboratory, Madison, US to study the effect of rate of loading on the bending and compression parallel to the grain, Liska [2]. The planks were small in size and free of defects and as straight grained as possible. Loading times ranged from 0.3 to 150 seconds. The bending tests were performed in a hydraulic testing machine with a constant head movement. Some of the results are shown in Figure 1. The average of the controls (reference) mentioned in Figure 1 refer to the standard bending tests of Maple. The data for all wood species follow the same tendency. At the highest loading rate the strength is about 20 to 30% higher than the standardised bending strength. More recently Madsen et. al. [3] and Jansson [4] studied the impact bending strength on simply supported timber beams by dropping a weight from various heights. The three-point loading was accomplished by a fit to purpose built machine, Figure 2. The drop height of the 345 kg weight varied from 50, 150 and 300 mm height resulting in a maximum impact velocity of 2,3 m/s. The average times to failure were 25, 17 and 10 milliseconds. Essential in these tests by Jansson [4] is that the impact force was measured directly by means of a load cell between the drop weight and the test specimen. In the analyses of the results the importance of separating the applied load in a part, which introduce bending stresses and a second part, which sets the beam into motion, is demonstrated. It should be pointed out that previous researchers ignored inertia forces as they were assumed negligible. Analytical procedures earlier developed by Bentur et al. [5] to estimate the inertia effect were explored but rejected. Jansson [4] turned to a Modal Analysis approach to tackle this problem. Some of his experimental results are given in Figure 3 where on the vertical axes the ratio of the impact and static bending strength is given.

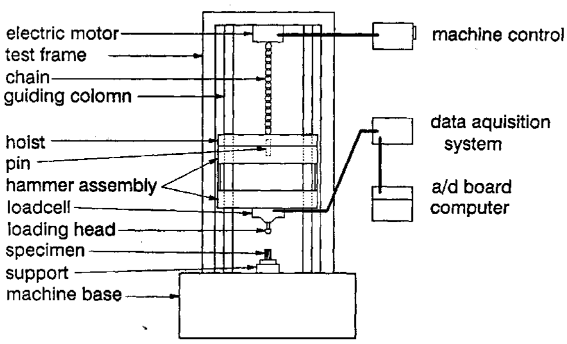

Figure 2: Test set-up by Madsen et al. (1986) and Jansson (1992)

The impact bending strength decreases with decreasing time to failure. The deviation from the test results mentioned earlier is considerable. No strength increase of 20 to 30% but a strength decrease of 15% for the shortest loading time of 10 milliseconds was observed when the inertia forces are taken into account.

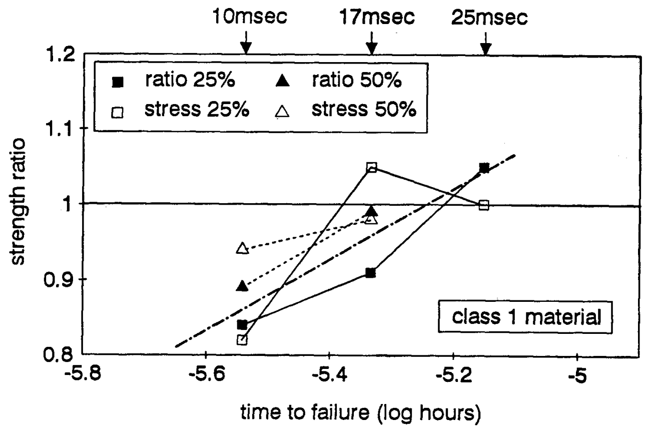

Figure 3: Final results of impact tests by Jansson (1992)

3 Aim of the impact tests, test apparatus and test specimens

The aim of the research was to detect differences in bending strength comparing results of standard bending and impact bending tests.

3.1 Rate of impact loading

In the guard-rail test standard EN 1317 a number of performances levels are specified. The performance level H2 of the Dutch guard-rail was arbitrarily set by the authorities. The two tests prescribed for H2 level are full-scale crash tests with a heavy 18-ton bus and a car. The bus shouldn't break through the structure while for the car test the acceleration of the passengers is limited. As the bus crash tests is regarded as the governing test case for strength the loading speed in the impact tests was deduced from this test. The bus entrance speed is 70 km / h (19.4 m / s). It will hit the guard rail at an angle of 20^0 as prescribed by the EN 1317, which leads to a lateral speed of 19.4 sin 20^0= 6.7 m / s. For this reason a load speed of 7.0 m / s was chosen in the impact test.

3.2 The test apparatus and instrumentation of the specimens

In principle the test apparatus compares well with Figure 2 accept for the loading head. The drop weight consisted of two cubic pieces of solid steel placed on both sides of a solid steel rod that acted as loading head. To prevent indentation of the timber test piece the rod diameter was arbitrarily set to 110 mm. The total weight of the drop piece was 199.0 kg.
The specimen was simply supported with a span of 1400 mm, and loaded by the drop-weight at mid span. Near the supports special devices were set up as prevent up lifting and to support any unstable specimens at time of failure. The weight was instrumented with an accelerometer. The de-acceleration of the drop weight, thought to be a key to determine the excitation force didn't work. The shock waves in the weight itself overruled the de-accelerating signal completely. A transducer (LVDT) attached to the bottom side of the timber specimen directly underneath the impact location, Figure 4, took the beam deflection. This LVDT was hidden in a stronghold below the specimen to prevent any damage of the device after failure of the specimen. A high-speed video camera (9000 frames per second or one frame every 0.111 ms) enabled monitoring the behaviour during the test. The high-speed camera appeared to be of vital importance in the determination of the time to failure. Failure was defined as the visual appearance of the first crack.

Figure 4: Transducer attached to specimen

3.3 The specimens

The number of specimens per wood species was limited to twenty per wood species. Seven wood species were selected for the experiments, Angelim Vermelho (tropical hardwood), Douglas Fir, Ash, Larch and three so-called heat threaded or heat modified wood species. Angelim Vermelho was the wood species to be used in the actual build guard rail system while Larch and Ash were regarded as good shock absorbers from literature. The only heat treated wood species currently available on the market were chosen. With the PLATO process Douglas Fir was modified (PLATO is a Dutch patented process) while Spruce (Picea Abies) and Pine (Pinus Silvestries) were modified using the Finnish STELLAC process. Clear free were Angelim Vermelho, Douglas Fir and Ash while the others were of a commercial grade including knots and other deficiencies. The PLATO wood was of the lowest grade involving the biggest knots. All specimens were conditioned at 80% RH and 20^0 C until equilibrium was obtained. The batches for standard bending and impact were matched on the basis of the MOE**.**

4 Bending tests

4.1 Static bending

The loading procedure corresponded with EN 408. The specimens of about 1600 mm length are symmetrically positioned on the supports of 1400 mm span and loaded until failure. The load deflection curve is recorded as well as signal of the accelerometer.

4.2 Impact bending tests

The high-speed video camera recordings with 9000 frames/second showed a phenomenon worth mentioning here and appeared to be of importance for the simulations and interpretation of the test results. The pictures clearly showed that after an initial phase of impulse transfer the beam accelerated rapidly and lost contact with the drop-weight. The impulse transfer was apparently so high that the beam speeded up more than the drop-weight fell. After a short time the drop-weight made contact again and transferred a second impulse. The second separation between both was much smaller and shorter than the first time. Finally, the drop-weight established a permanent contact and worked its way down until failure of the beam occurred. In Figure 5 both output signals are given. The horizontal curve (not smooth) near the bottom resembles the output signal of the accelerometer and the second one (smooth) is the deflection. On the left axis the deflection in given in millimetres. Time is set to zero at first contact. The bouncing effect mentioned above is proven by this deflection curve. Certainly the first bump in this curve is clearly visible. Janssen [4] showed that the previous applied analytical method to determine the bending stresses from the experimental data was questionable. In pursue of a more reliable method a computer simulation programme was adopted. The tuning of the simulation programme to fit the recorded test data is obviously very important. In this programme the inertia influences are taken into account in a more accurate way than possible by the analytical methods.

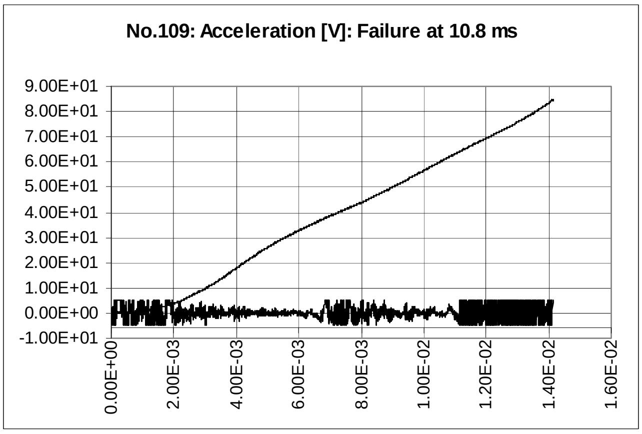

Figure 5: Deflection [mm] versus time [s] at the bottom the accelerometer signal

5 The simulation model

The FEM simulation model is based on Thimoshenko elements. A. Kok [5] developed this particular simulation model suited to load the beam by impulses and to attach lumped masses at any given time. The model accounts for all inertia effects. A single impulse at the beginning of the simulation represents the initial contact and after a given time the drop-weight characterised as a lumped mass of a certain quantity and velocity can be attached to the mid span elements. Damping can be introduced to diminish the effect of higher order vibrations.

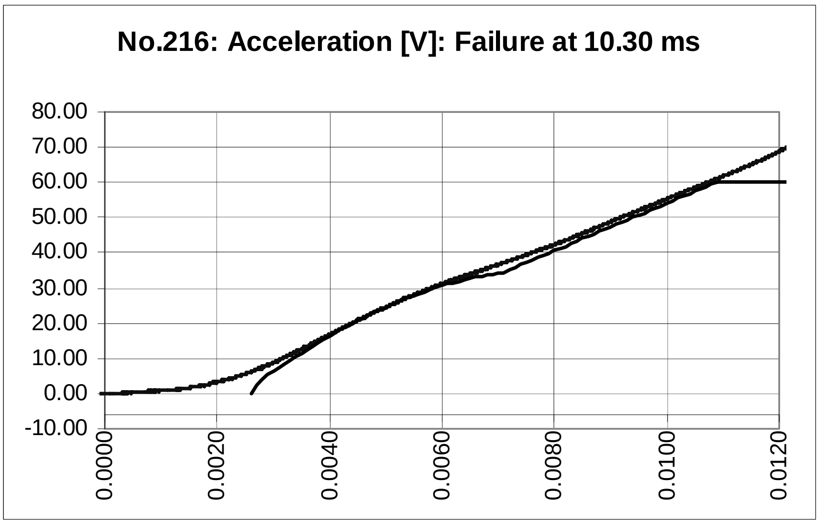

Figure 6: Test and simulation results of deflection [mm] versus time [s]

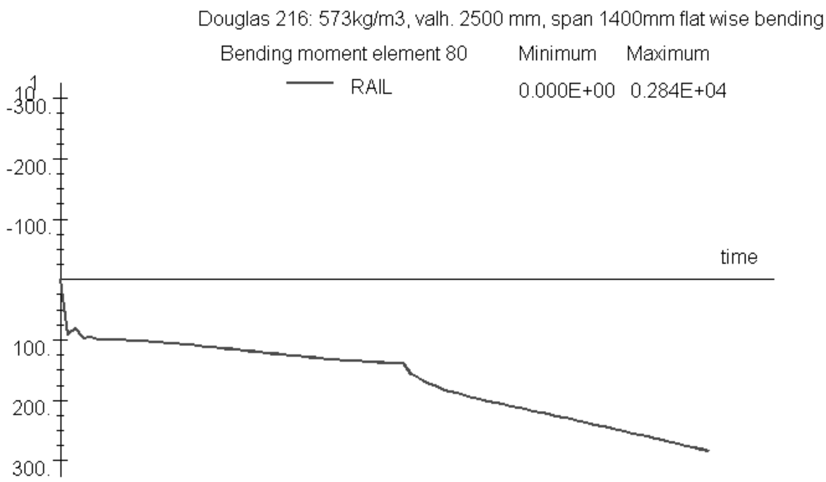

Figure 7: Simulated bending moment [Nm] versus time [s] at mid span

The 1600 mm long beam consisted of 160 elements of 10 mm each. The beam supports allowed rotation but no up-lift. For every specimen the relevant material properties, MOE, density and dimensions were part of the input file. The simulation generated deflection, rotation, bending moments and shear forces. It allowed plotting the simulated time deflection curve together with the time deflection graph recorded, Figure 6. The test starts at t = 0. As Figure 6 shows in the first 2 ms not only the beam needs time to accelerate also the deflection apparatus needs time to keep up with the sudden signal change. Obviously, the mathematical beam in the simulation exposed to an impulse reacts immediately. To have agreement between both curves the initial contact in the simulation is delayed. The delay time and the initial impulse are chosen such that both experimental and simulation time deflection curve are in good agreement.

Having set the simulation input variables such that the deflection versus time corresponds well with the test data the model generates the corresponding bending stresses at any location along the beam. The overall majority of beams failed at mid span. For that reason the mid span bending moment was taken as the governing value for the derivation of the bending strength. Only in some cases knots and slope of grain caused failure initiation a small distance from mid span. In Figure 7 a plot is given of a typical mid span bending moment versus time plot. The maximum bending moment is given in the top right corner in Nm. The bending stress is derived in the traditional way assuming Hook's law applies for these conditions. Regarding the failure mode it was observed that nearly all specimens, some specimens failed because of knots outside the centre area, failed showing shorter fibres for the impact tests. No conclusion could be drawn regarding the influence of the heat treatment as this parameter was not included in the test programme.

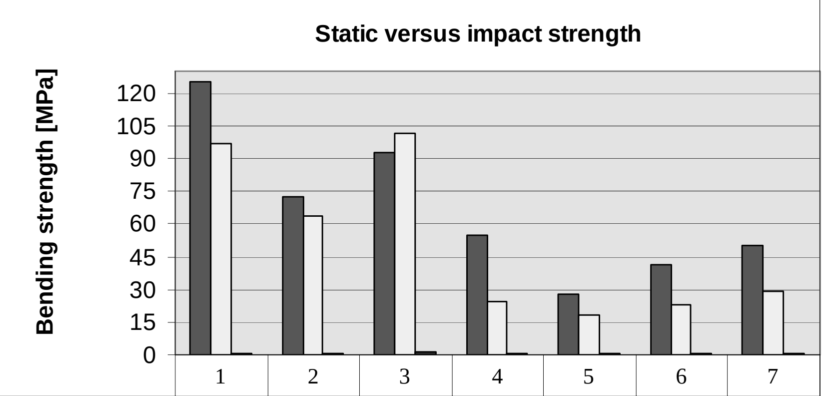

	1	2	3	4	5	6	7
Standard	125.2	72.2	92.8	55.1	27.7	41.4	50.1
Impact	96.7	63.8	101.6	24.3	18.3	23.3	28.8
Impact/Standard	0.77	0.88	1.09	0.44	0.66	0.56	0.57

*)Column numbers correspond with Table 1 column 1 values in brackets

Figure 8: Overview of the impact and static strength results

6 Evaluation of the results

The results are graphically represented in Figure 8. The strength ratio impact bending / standard bending is given in the lower part of Figure 8. Notices the ratio in Column (3) for Ash, which is higher than 1, while for all other wood species it is considerable smaller than 1.
In Table 1 the results of the simulation are presented per wood species and complimentary the data of the standard bending tests is added. To drawn more reliable conclusions only based on differences in mean bending strength the statistical t-test was applied. This allows checking whether or not the differences in mean strength are significant (significance level 5%). The analysis concludes that with 95% certainty the mean bending strength of Angelim Vemelho, Larch, Mod. I., Mod. II and Mod III wood species in impact bending is indeed significantly different from the standard bending strength. No significant difference was found for Douglas Fir and Ash.

Table 1: Results of standard and impact strength tests

(1) Wood species	**(2)** number of tests n	**(3)** Standaard bending [Mpa]	**(4)** c.o.v. [%]	**(5)** number of tests n	**(6)** Impact bending [Mpa]	**(7)** c.o.v. [%]
Angelim Vermelho (1)	11	125.2	13	10	96.7	38
Douglas Fir (2)	10	72.2	14	10	63.8	39
Ash (3)	4	92.8	9	7	101.6	12
Larch (4)	11	55.1	26	10	24.3	29
Mod.I (5)	12	27.7	23	11	18.3	37
ModII (6)	13	41.4	24	22	23.3	20
Mod III (7)	17	50.1	24	14	28.8	27

The difference between standard static and impact strength has some relation with grade quality as the wood species of commercial grade (containing knots) reduced more in strength than others. Apart from Ash the other wood species free of any knots such as Angelin Vermehlo and Douglas Fir, dropped in strength only 23 and 12% respectively. The other wood species with knots such as Larch and the heat-treated wood species dropped 40 to 60 % in strength. The influence of knots turns out to be of significant importance. This agrees with the conclusion by Jansson [4] that commercial timber behaves worse than clear and free wood specimens.

7 Summary and conclusions

Standard and impact bending tests have been performed on matched timber specimens in flat wise three point bending. The span was 1400 mm while the specimens had a cross-section of about 40x130 mm. Seven wood species were investigated Angelim Vermelho, Douglas Fir, Ash, Larch and three heat modified wood species of Pine, Spruce and Douglas. The number of specimens per wood species in the static and impact test was 10 with some exceptions.
The standard bending tests were performed according to EN 408. For the impact tests a tailor made apparatus was built in absents of any standardised apparatus. The load application consisted of a 199 kg drop-weight, which fell from 2.5m height and reached a speed at impact of 7 m/s. During impact the deflection was recorded at mid span. Failure was defined as the occurrence of the first crack. A high-speed camera (9000 frames a second) was used to record the time to failure. In order to determine the bending strength a simulation programme was used. The dynamic programme was tuned in such a way as to simulate the most important phenomenon observed during the impact test up to failure.
Reviewing the strength values derived it was concluded that the mean impact bending strength is in most cases lower than the static bending strength. It was concluded that no significant bending strength difference could be demonstrated for Ash and Douglas Fir. However, all other wood species especially those of commercial grade (containing knots) showed a considerable reduction in strength from 40% up to 60%. Despite the low number of tests the conclusions are in line with the results of Jansson [4].

Acknowledgement
Thanks to the laboratory staff of Steel&Timber structures of the Civil Engineering Faculty of TU-Delft. Especially, Hylke Katsma and P. Stolle for their assistance in testing and active participation in solving all practical problems. I also want to express my thanks to Dr. A. Kok for his stimulating help using his simulating programme. Furthermore, I would like to acknowledge the ministry of Traffic and Waterways DWW and Centrum Hout for their financial support in financing this research project. Also Wittpress is acknowledged for their permission using some parts of [6].

References

[1] Bodig, J. and Jayne, B. A., Mechanics of wood and wood composites, ISBN 0-442-00822-8, Van Nostrand Reinhold Company,1982

[2] Liska, J.A., Effect of rapid loading on the compressive and flexural strength of wood, Report 1767, Forest Products Laboratory, Forest Service, Madison, Wisconsin, 1955

[3] Madsen,B and Mindess, S., The fracture of wood under impact loading, Material and Structures, Vol. 19, No. 109. 1986

[4] Jansson, B., Impact loading of timber beams, M.Sc. thesis, Faculty of Civil Engineering, University of British Columbia, April.1992.

[5] Kok, A. 1997, Lumped impulses, discrete displacements and moving load analysis, HERON 1997, vol.42, No. 1, p.3 -23, ISSN 0046-7316

[6] Leijten, A.J.M., 2001, Impact crash and simulation of timber beams, In: Proc. of 10th Int. Conference on Computational Methods and Experimental Measurements, Wittpress, Southampton.